c1

IDENTIFICATION OF A $^1\Delta_u - {}^1\Sigma_g^+$ TRANSITION OF CS_2 IN THE NEAR ULTRAVIOLET

by

DAVID NELSON MALM

B.Sc., University of British Columbia, 1970

A THESIS SUBMITTED IN PARTIAL FULFILMENT OF
THE REQUIREMENTS FOR THE DEGREE OF
MASTER OF SCIENCE

In the Department
of
Chemistry

We accept this thesis as conforming to the
required standard

THE UNIVERSITY OF BRITISH COLUMBIA

October, 1972

In presenting this thesis in partial fulfilment of the requirements for an advanced degree at the University of British Columbia, I agree that the Library shall make it freely available for reference and study. I further agree that permission for extensive copying of this thesis for scholarly purposes may be granted by the Head of my Department or by his representatives. It is understood that copying or publication of this thesis for financial gain shall not be allowed without my written permission.

Department of CHEMISTRY

The University of British Columbia
Vancouver 8, Canada

Date October 6, 1972

ABSTRACT

The strongest features in the absorption spectrum of CS_2 in the region 2900Å to 3500Å are identified, from temperature studies, as a $\pi \rightarrow \pi^*$ $^1\Delta_u - {}^1\Sigma_g^+$ transition, where the Renner-Teller effect has split the $^1\Delta_u$ state into $^1B_2$ and $^1A_2$ component states of a bent molecule. Analysis of some of the least severely perturbed bands of the $^1B_2 - {}^1\Sigma_g^+$ transitions (3300 - 2900Å) shows that they form a parallel-polarized progression in the bending vibration, to an upper state with r(C - S) = 1.54_4Å, $<S\hat{C}S \simeq 163°$, and a barrier to linearity of ~ 1400 cm^{-1}. Two hitherto unrecognized progressions of 'hot' bands, a weak vibronic $\Pi - \Pi$ and a stronger vibronic $\Delta - \Delta$ progression in the region 3300Å to 3500Å, are assigned to the $^1A_2 - {}^1\Sigma_g^+$ transiton. This is a new type of transition, which does not appear in cold absorption, but whose 'hot' bands can obtain an amount of intensity (proportional to K^2) through Renner-Teller mixing.

TABLE OF CONTENTS

List of Tables and Figures

ACKNOWLEDGMENT

The author wishes to thank his research supervisor, Dr. A.J. Merer, as well as Dr. Christian Jungen, for their advice and encouragement in the research upon which this thesis is based. A special word of thanks is also due E.M. who gave much needed support throughout the 'dog days' of thesis writing and to Rose Chabluk for her fine job in the typing of this thesis.

I. INTRODUCTION

Carbon disulfide has a complex electronic absorption spectrum in the visible and ultraviolet regions. In the region 4300Å to 2900Å there are several relatively weak systems (1-6), and in the region 2300Å to 1800Å (7-8) there are several systems of much stronger absorption. A number of intense bands between 1850Å and 1375Å (7) (probably belonging to several electronic transitions) have not been analysed. From 1375Å to 600Å Rydberg series converging to the CS_2^+ ionization limits have been characterized (9-10).

The electronic configuration of CS_2 in its electronic ground state is

$$\ldots (\sigma_g)^2 \quad (\sigma_u)^2 \quad (\pi_u)^4 \quad (\pi_g)^4 \qquad {}^1\Sigma_g^+$$

CS_2 is linear in the ground electronic state with a C-S bond length of 1.554_5Å (11-12). The shape and bonding characteristics of the filled and unfilled orbitals available to CS_2 are discussed by Walsh (13). The lowest energy excited electron configuration is $\ldots (\pi_g)^3 (\pi_u^*)^1$ where π_u^* is an anti-bonding orbital. The configuration gives rise to ${}^1\Sigma_u^+$, ${}^1\Sigma_u^-$, ${}^1\Delta_u$, ${}^3\Sigma_u^+$, ${}^3\Sigma_u^-$ and ${}^3\Delta_u$ states. Only one of the possible $\pi \rightarrow \pi^*$ transitions is fully allowed by the spin and orbital symmetry selection rules, and this has been identified with the strong 2100Å absorption bands (13). A rotational analysis of a few of the 2100Å bands (14) showed the transition to be parallel-polarized, ${}^1B_2 - {}^1\Sigma_g^+$, going to an upper state in which CS_2 is slightly bent with an S-C-S bond angle of 153° and a C-S bond length of 1.66Å. The vibrational structure is not

well understood, though there is no doubt that the upper electronic state is the $\pi \rightarrow \pi^*$ $^1B_2$ ($^1\Sigma_u^+$) state.

In the region 3800Å to 3300Å Liebermann (4) found six vibrational bands to have $^1\Sigma$ - $^1\Sigma$ -type rotational structures. More recently, Kleman (15) showed that the absorption in the region 4300Å to 3300Å consists of two electronic systems. In the lowest excited electronic state, which he called the R state, the molecule is bent, with an S-C-S bond angle of 135.8° and a C-S bond length of 1.66Å. A long progression in the bending frequency, $\nu_2' = 311$ cm^{-1}, and a shorter progression in the symmetric stretching frequency, $\nu_1' = 691.5$ cm^{-1}, were assigned, as well as numerous 'hot' bands from excited vibrational levels of the ground electronic state. Kleman was unable to identify the electronic state of the $\pi \rightarrow \pi^*$ excitation responsible for the R system except to say that the R system was parallel-polarized, with a B_2 upper state.

Although the R bands are singlet in appearance, the magnetic rotation spectrum (16) and the Zeeman effect (17) indicate that the R state is actually a triplet state. The lowest triplet electronic state, as predicted by theoretical considerations (13,18), is the $^3\Delta_u$ ($\pi \rightarrow \pi^*$) state. In the bent molecule the orbital degeneracy of the $^3\Delta_u$ electronic state is lifted, giving rise to $^3A_2$ and $^3B_2$ component states. More comprehensive Zeeman effect studies (19), as well as theoretical calculations (20), assigned the R state as a Hund's coupling case (c) spin multiplet sub-component (B_2) of a $^3A_2$ electronic state. The Zeeman

spectrum of solid CS_2 at 4.2°K (21) showed weak magnetic field induced absorption to the other two spin multiplet sub-components (A_1, B_1) of the $^3A_2$ state, 36 cm^{-1} to the red of the B_2 sub-component responsible for the R system. As predicted by Hougen (20), this observation is consistent with the $^3A_2$ ($^3\Delta_u$) component state lying lower in energy than the $^3B_2$ ($^3\Delta_u$) component state.

Kleman identified a second electronic system (which he called the S system) in the region 3700Å to 3350Å; this consists of another parallel-polarized progression in the upper state bending frequency, $\nu_2' = 270$ cm^{-1}. The rotational structure of the vibrational bands is simple, like that of the R bands.

The strongest CS_2 absorption in the near-ultraviolet, in the region 3400Å to 2900Å, was called the V system by Kleman. The complexity of the V system has so far prevented a vibrational or rotational analysis. Recently, however, the absorption spectrum of the V system was observed in matrices at 20°K and 77°K by Bajema, Goutermann and Meyer (22), who found a considerable simplification of the vibrational structure in the matrix over the gas phase spectrum. The matrix spectrum consists essentially of a single progression of 580 ± 30 cm^{-1}, which they assigned as the symmetric stretching vibration of a molecule linear in the upper state. The complexity of the V state was attributed to the effects of Renner-Teller interaction in a $^1\Delta_u$ electronic state of a linear molecule. However, the conclusion reached in this thesis is that the 580 cm^{-1} interval corresponds to the bending vibration of a bent molecule with a $^1B_2$ ($^1\Delta_u$) upper state.

II. EXPERIMENTAL

Low resolution survey spectra of CS_2 were taken on a Cary 14 recording spectrophotometer. A 10 cm cell was filled with CS_2 vapour to 4 cm pressure and then opened to the air to give a pressure-broadened spectrum.[†] Without pressure-broadening, all absorption bands of width less than the resolution of the Cary 14 would be recorded with incorrect intensities.

Medium resolution gas phase spectra (approximately 150,000 resolving power) were photographed in the second order of a 21 ft focal length Eagle-mounted concave grating spectrograph. Quartz gas cells fitted with Suprasil windows were used to give path lengths of 80 cm and 160 cm. It was necessary in all experiments to use a Corning 7-54 filter to remove wavelengths of less than 2300Å from the incident radiation to prevent photodissociation of CS_2 (23) according to the reaction

$$CS_2 \xrightarrow{h\nu} CS(A^1\Pi) + S(^3P_2)$$

This reaction is energetically possible at wavelengths less than 2778 ± 10Å, but because there is almost no absorption from 2800Å to 2300Å, decomposition is troublesome only with incident light of wavelength less than 2300Å. With a 20μ slit and CS_2 pressure ranging from

[†]All pressures will be quoted in units of cm or mm of Hg.
1 mm Hg = 133.32 N/m^2.

0.2 mm to 5 mm, exposure times were of the order of 10 sec using Kodak SA-1 plates. Wavelength calibration for all spectra photographed was with a 120 ma iron-neon hollow-cathode lamp of the lab's own design.

The temperature dependence of the near-ultraviolet bands was investigated by photographing spectra of CS_2 at -78°, 23°, 85°, 100° and 200°C. Elevated temperatures were achieved by wrapping the cell with electric heating tape over which was wound asbestos cloth insulation. Varying the applied voltage on the heating tape gave the desired temperature. As measured with a mercury thermometer next to the cell surface, a regulation of ±2°C was achieved.

To compare relative intensities of bands as a function of temperature, the number of absorbing molecules in the light path had to be kept constant at the different temperatures. This presented no problem except at -78°C, for, even at room temperature, the vapour pressure of CS_2 is $\sim$ 300 mm, far in excess of the pressure needed to obtain sufficient absorption. However, at -78° the vapour pressure of CS_2 is only 0.2 mm. Since the near-ultraviolet absorption is comparatively weak, this necessitated the use of very long absorption path lengths. Using a 4 m White-type multiple reflection cell (24,25) of the lab's own design (as shown in Fig. 1), path lengths of up to 128 m could be attained. The cell consists of 85 mm pyrex tubing, to the ends of which ordinary pyrex pipe flanges are attached. Steel end-plates sealed by 'O' rings are secured to the flanges to produce a vacuum seal. One

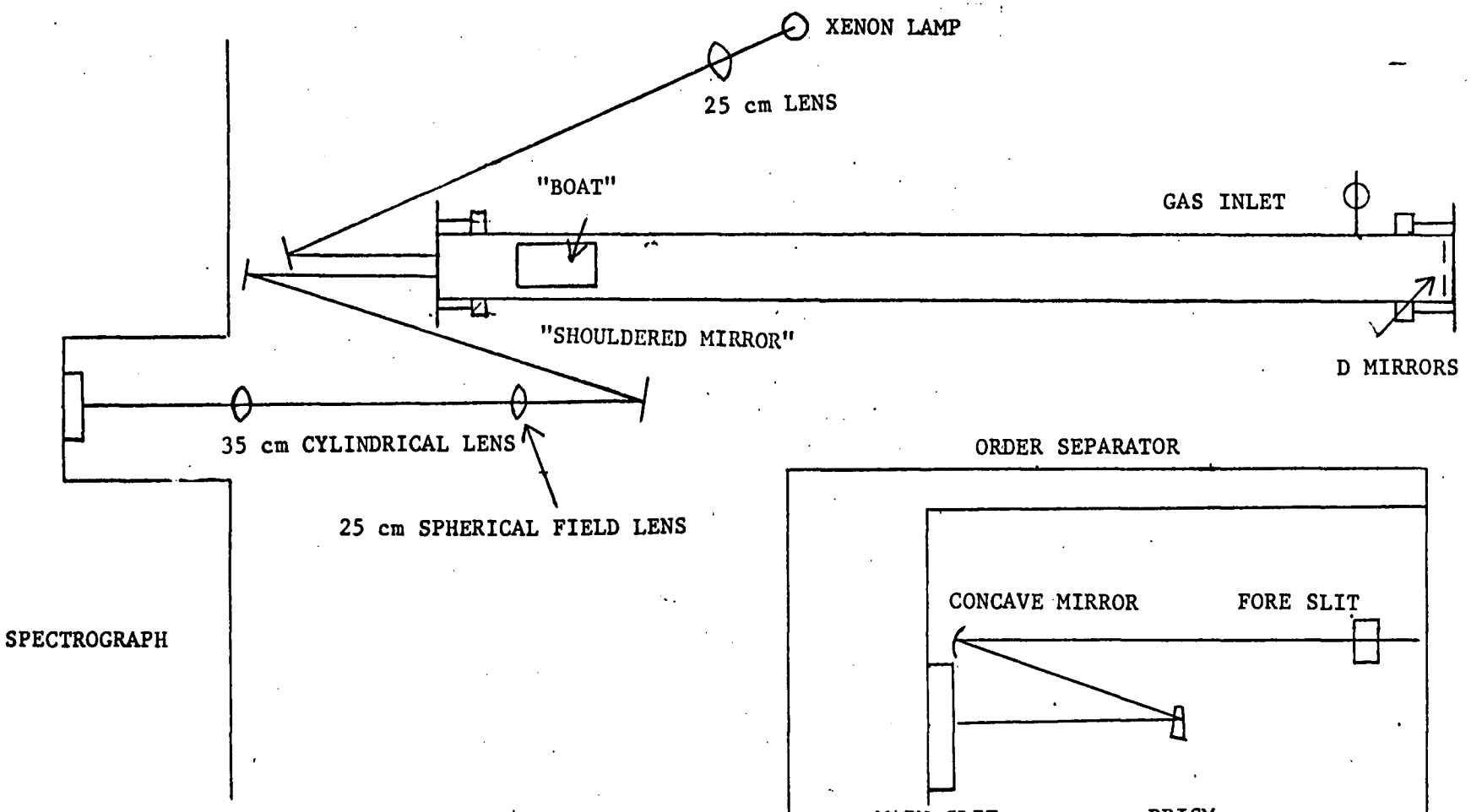

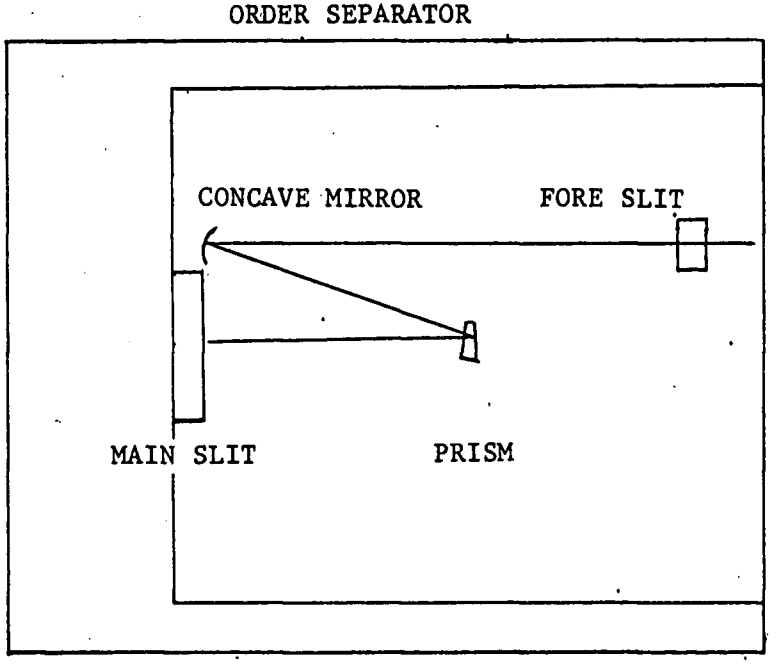

FIG. (1) 4 Meter White Cell and Order Separator

end-plate carries the Suprasil entrance and exit windows, while the other end-plate has external controls for the concave 'D'-shaped mirrors. Inserted in the cell near the quartz windows is a 'boat' which holds in position the shouldered circular concave mirror. The number of traversals of the cell (multiples of 4) was controlled by manipulation of one of the D mirrors.

For temperature studies at -78°C, dry ice was packed between the White cell and its styrofoam-insulated box. To attain elevated temperatures, the White cell was wrapped with heating tape and insulating asbestos cloth. Due to the large mass of pyrex tubing, a temperature of only 85 ± 5°C was possible. With the White cell set for 12 traversals (∿48 m path length), a CS_2 pressure at -78°C of 0.2 mm and a 30μ slit width, exposures on the Eagle spectrograph were about 10 minutes with Kodak SA-1 plates.

High resolution spectra (approximately 625,000 resolving power) were photographed in the $16^{th.}$ - $19^{th.}$ orders of a 7 m focal length Ebert-mounted plane grating spectrograph. To prevent an overlapping of spectral orders, an order separator consisting essentially of a small quartz prism monochromator was placed between the spectrograph (main) slit and the external optics (Fig. 1). By rotating the Suprasil quartz prism, the wavelength of light falling on the main slit could be varied. By adjusting the fore-slit width between 100μ and 1500μ, the 'bandpass' admitted could be varied from approximately 40Å to 300Å. With the White cell set for 12 traversals, a fore-slit width

of 400μ and a main slit width of 20μ, exposures of about 10 minutes were required with Kodak SA-1 plates. Calibration of the high resolution spectra was achieved by increasing the order separator bandpass so that several orders adjacent to the molecular spectral order were photographed. This is necessary because at the high dispersion of the Ebert spectrograph (0.137Å/mm in $17^{th.}$ order) the density of iron calibration lines in any one order is not sufficient for accurate interpolation between them.

CS_2 (Fisher RG) was used without further purification except for de-gassing under vacuum at liquid nitrogen temperature. The standard all glass vacuum line used a dual chamber rotary pump and an oil diffusion pump. Gas pressures were measured with a thermocouple gauge and with a manometer filled with Dow Corning 707 silicone fluid (12.8 mm silicone oil = 1 mm Hg). Dow silicone high vacuum stopcock grease, used throughout the vacuum line, was the only grease that resisted formation of bubbles of dissolved CS_2. An ultimate vacuum of 0.001 mm was routinely achieved with all absorption cells. The gas cells were filled to the desired pressure simply by allowing the frozen, de-gassed CS_2 to warm slowly, liquefy and evaporate.

The high resolution plates were measured on a Grant automatic recording photoelectric comparator in the Physics Department, and all the measurements were reduced to vacuum wavenumbers by means of a computer programme that performed a least squares fit of the iron and neon reference line wavelengths (26) to a 4-term polynomial. It is

estimated that relative positions of unblended lines are accurate to better than ± 0.01 cm^{-1}.

Band head positions used in the vibrational analysis were measured from high contrast photographic enlargements of the medium resolution plates. Interpolation between two close reference lines provided a relative band head accuracy of ± 1 cm^{-1}.

III. THEORY

A. Symmetry Properties of CS_2

The point group of linear CS_2 is $D_{\infty h}$ and that of bent CS_2 is C_{2v}; their character tables are given as Table I. The labelling of the symmetry axis is different for the two point groups because, according to Mulliken's convention (27), the z axis is the molecular axis for the linear molecule, but the two-fold rotation axis (C_2) for the bent molecule. When linear CS_2 becomes bent, all symmetry operations of $D_{\infty h}$ not retained in C_{2v} are no longer defined. The correlation of symmetry operations between $D_{\infty h}$ and C_{2v} is as follows: C_2', the one remaining rotation about an axis perpendicular to the linear axis becomes the $C_2(z)$ rotation in the C_{2v} point group; σ_h, reflection in a plane perpendicular to the linear axis becomes $\sigma_v(xz)$; similarly, the one remaining reflection, σ_v, becomes $\sigma_v(yz)$. All other $D_{\infty h}$ operations are undefined, including the inversion operation, so that the 'g,u' species designations of the linear molecule are undefined for the bent molecule. The resulting correlation of species is given as Table II.

The axis correlation for $D_{\infty h}$ with C_{2v} is as follows: $x \leftrightarrow x$, $y \leftrightarrow z$, $z \leftrightarrow y$. The linear molecule non-degenerate point group species correlate in a one-to-one manner with the C_{2v} point group species. However, all other $D_{\infty h}$ species are doubly degenerate and correlate with A + B species of C_{2v}. That is, the correlation of symmetry species is unique only when the symmetry is lowered upon bending the linear molecule; the correlation is ambiguous when bent CS_2 becomes linear.

TABLE I

$D_{\infty h}$ and C_{2v} Point Groups

$D_{\infty h}$	I	$2C_\infty^\phi$	$2C_\infty^{2\phi}$	$2C_\infty^{3\phi}$	...	∞C_2	σ_h	$\infty\sigma_v$	$2S_\infty^\phi$	$2S_\infty^{2\phi}$	...	$S_2 \equiv i$	
Σ_g^+	1	1	1	1	...	1	1	1	1	1	...	1	
Σ_u^+	1	1	1	1	...	-1	-1	1	-1	-1	...	-1	z
Σ_g^-	1	1	1	1	...	-1	1	-1	1	1	...	1	R_z
Σ_u^-	1	1	1	1	...	1	-1	-1	-1	-1	...	-1	
Π_g	2	$2\cos\phi$	$2\cos2\phi$	$2\cos3\phi$	...	0	-2	0	$-2\cos\phi$	$-2\cos2\phi$	...	2	R_x, R_y
Π_u	2	$2\cos\phi$	$2\cos2\phi$	$2\cos3\phi$	...	0	+2	0	$2\cos\phi$	$2\cos2\phi$	...	-2	x,y
Δ_g	2	$2\cos2\phi$	$2\cos4\phi$	$2\cos6\phi$	...	0	+2	0	$2\cos2\phi$	$2\cos4\phi$	...	2	
Δ_u	2	$2\cos2\phi$	$2\cos4\phi$	$2\cos6\phi$	...	0	-2	0	$-2\cos2\phi$	$-2\cos4\phi$	...	-2	
Φ_g	2	$2\cos3\phi$	$2\cos6\phi$	$2\cos9\phi$	...	0	-2	0	$-2\cos3\phi$	$-2\cos6\phi$	...	2	
Φ_u	2	$2\cos3\phi$	$2\cos6\phi$	$2\cos9\phi$	...	0	+2	0	$2\cos3\phi$	$2\cos6\phi$	...	-2	
...	...	...	...	...	...	...	...	...	...	...	...	...	

TABLE I (continued)

C_{2v}	I	$C_2(z)$	$\sigma_v(xz)$	$\sigma_v(yz)$	
A_1	1	1	1	1	z
A_2	1	1	-1	-1	R_x
B_1	1	-1	1	-1	x, R_y
B_2	1	-1	-1	1	y, R_x

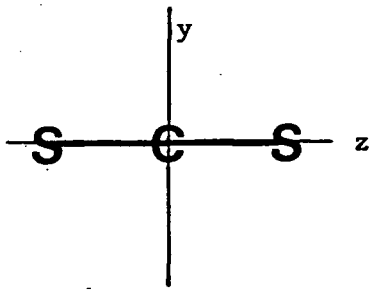

$D_{\infty h}$ point group axis system

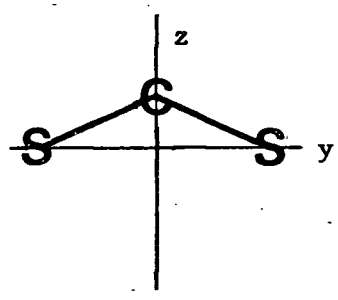

C_{2v} point group axis system

The x axis is out of the plane of the paper.

TABLE II

Correlation of Species of $D_{\infty h}$ and C_{2v} Point Groups

$D_{\infty h}$	Σ_g^+	Σ_u^-	Σ_g^-	Σ_u^+	Π_g	Π_u	Δ_g	Δ_u	Φ_g	Φ_u	...
C_{2v}	A_1	A_2	B_1	B_2	A_2+B_2	A_1+B_1	A_1+B_1	A_2+B_2	A_2+B_2	A_2+B_2	...

B. Vibrational Energy Level Patterns

In order to gain familiarity with the conventional spectroscopic nomenclature used throughout this thesis, a cursory development of the theory of vibration and rotation of a symmetric triatomic molecule will be outlined. We begin with a consideration of the theory of Normal Modes of vibration.

The three translational degrees of freedom possessed by each of the N constituent atoms become the translational, vibrational and rotational degrees of freedom of the molecule formed from these atoms. The number of vibrational degrees of freedom is thus 3N - 6, (or 3N - 5 for a linear molecule which has only two rotational degrees of freedom). It is very difficult to consider the vibrations of a polyatomic molecule using Cartesian displacement coordinates because the vibrational motions are quite closely identifiable as stretchings of bonds, bond angle changing motions, or twistings. For this reason it is customary to introduce Normal coordinates of vibration, which correspond to the actual motions of the atoms, with suitable mass-weighting. The detailed motions of the atoms are governed by the Force Field, a set of potential energy expressions containing the Force Constants and the Normal coordinates: these are conveniently written as a Taylor series in the 3N - 5(6) Normal coordinates

$$V = V_0 + \sum_k \left(\frac{\partial V}{\partial Q_k}\right)_0 Q_K + \frac{1}{2} \sum_k \sum_\ell \left(\frac{\partial^2 V}{\partial Q_k \partial Q_\ell}\right)_0 Q_k Q_\ell + \ldots \qquad (1)$$

With the choice of orgin as the 'Equilibrium Configuration' the first two terms may be removed, and the quadratic cross terms vanish because the Normal coordinates are defined to cause them to be zero. The potential energy is thus

$$V = \frac{1}{2} \sum_k \left(\frac{\partial^2 V}{\partial Q_k^2} \right)_0 Q_k^2 + \text{higher terms} \qquad (2)$$

If the higher terms are neglected, the Potential Energy is just a sum of quadratic terms, one for each vibration, k. This is analogous to the situation of a classical system undergoing simple harmonic motions, and is known as the 'Harmonic Approximation'.

The vibrational hamiltonian factorizes, in harmonic approximation, into a sum of one-dimensional hamiltonians, one for each vibrational motion

$$\hat{H} = \sum_k \left(\frac{1}{2} \hat{P}_k^2 + \frac{1}{2} \lambda_k \hat{Q}_k^2 \right) \qquad (3)$$

where the λ_k's are the Force Constants, i.e. $(\partial^2 V / \partial Q_k^2)_0$ and the $\hat{P}_k$'s are the momentum operators conjugate to the $\hat{Q}_k$'s. The eigenvalues of this hamiltonian, the 'Harmonic Oscillator' hamiltonian, are well-known (28,29) to be

$$E = \sum_k (v_k + \frac{1}{2}) \, h \, \nu_k \qquad \text{joules} \qquad (4)$$

where the v_k's are non-negative integers, and the ν_k's are related to the Force Constants by

$$\lambda_k = 4\pi^2 \nu_k^2 \qquad (5)$$

It is customary to define the quantity $\omega_k = \nu_k/c$, so that, in cm^{-1} units, the vibrational energy levels are

$$E/hc = \sum_k (v_k + \frac{1}{2})\ \omega_k \qquad cm^{-1} \qquad (6)$$

The effects of the cubic and higher terms omitted from the hamiltonian are to add corrections to this expression, called Anharmonicity Terms.

A linear symmetric triatomic molecule has 3N-5 = 4 vibrations, but two of these correspond to identical bending motions executed at right angles, and therefore have the same frequency ν; these are said to be 'degenerate' and one speaks loosely of the molecule as "having three vibrations, one of which is degenerate". The other two vibrations correspond to symmetric and antisymmetric combinations of the stretchings of the two bonds.

The vibrational energy level pattern is still given by equation (6), with the summation running over both components of the degenerate bending vibration. There is, however, an additional property associated with the bending vibration, which is the vibrational angular momentum. Physically its origin may be visualised as follows. In a normal vibration all the atoms move with the same frequency so that the Cartesian components of the displacements change according to sine curves. The superposition of two identical bending motions of equal amplitude at right angles and with a 90° phase shift results in the motions of the individual atoms describing a circle about the linear axis as illustrated below.

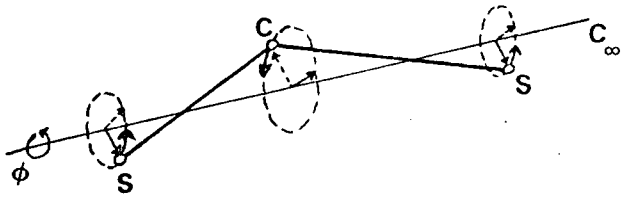

Such an addition of two harmonic motions at right angles resulting in rotation about the linear axis is equivalent to imparting an angular momentum to the nuclei with the vector of the vibrational angular momentum along the linear axis. The individual atoms execute a full rotation about the linear axis at the frequency of the degenerate bending vibration.

In mathematical terms the vibrational angular momentum arises because it is convenient to transform from Normal coordinates to cylindrical polar coordinates, when the product of two one-dimensional harmonic oscillator eigenfunctions becomes an Associated Laguerre function multiplied by an angular factor, $(1/\sqrt{2\pi})e^{i\ell\phi}$. This angular factor, as is well known (31), corresponds to an angular momentum in a system with axial symmetry. The notation used for a bending vibration is that the eigenfunctions are described by quantum numbers v_2 and ℓ, where v_2 is the sum of one dimensional oscillator quantum numbers, and ℓ is the vibrational angular momentum quantum number, which (from the properties of the Associated Laguerre function) may take the values v_2, $v_2-2,\ldots,-v_2$. As we show below, it is convenient, for rotational

energy level calculations, to define the vibrational angular momentum operator, $\hat{\underset{\sim}{G}}$. The eigenvalue of its z-component is, of course, $\ell(\hbar)$, i.e.

$$\hat{G}_z|v_2\ell\rangle = \ell\hbar|v_2\ell\rangle \qquad (7)$$

Anharmonic terms cause components of a vibrational level v_2 with different values of $|\ell|$ to lie at slightly different energies. The vibrational levels are classified as Σ, Π, Δ, ... according to whether $|\ell| = 0, 1, 2, \ldots$. In fact, any angular momentum states are classifiable in this manner.

The lowest vibrational levels of the ground state of CS_2 are given in Table III and illustrated in Fig. 2. The symmetric and antisymmetric stretching Normal vibrations are designated ν_1 and ν_3, with quantum numbers v_1 and v_3, respectively; the doubly degenerate bending vibration is labelled by the values of v_2 and ℓ. The species of the vibrational wavefunctions in the $D_{\infty h}$ point group are also given in Fig. 2. The notation $(v_1 v_2^{\ell} v_3)$ specifies the vibrational level of a linear symmetric triatomic molecule. The energy levels of the 'fundamentals' ($v_k = 1$) and the 'overtones' ($v_k = 2, 3, \ldots$) are shown, but the 'combination levels' are not given.

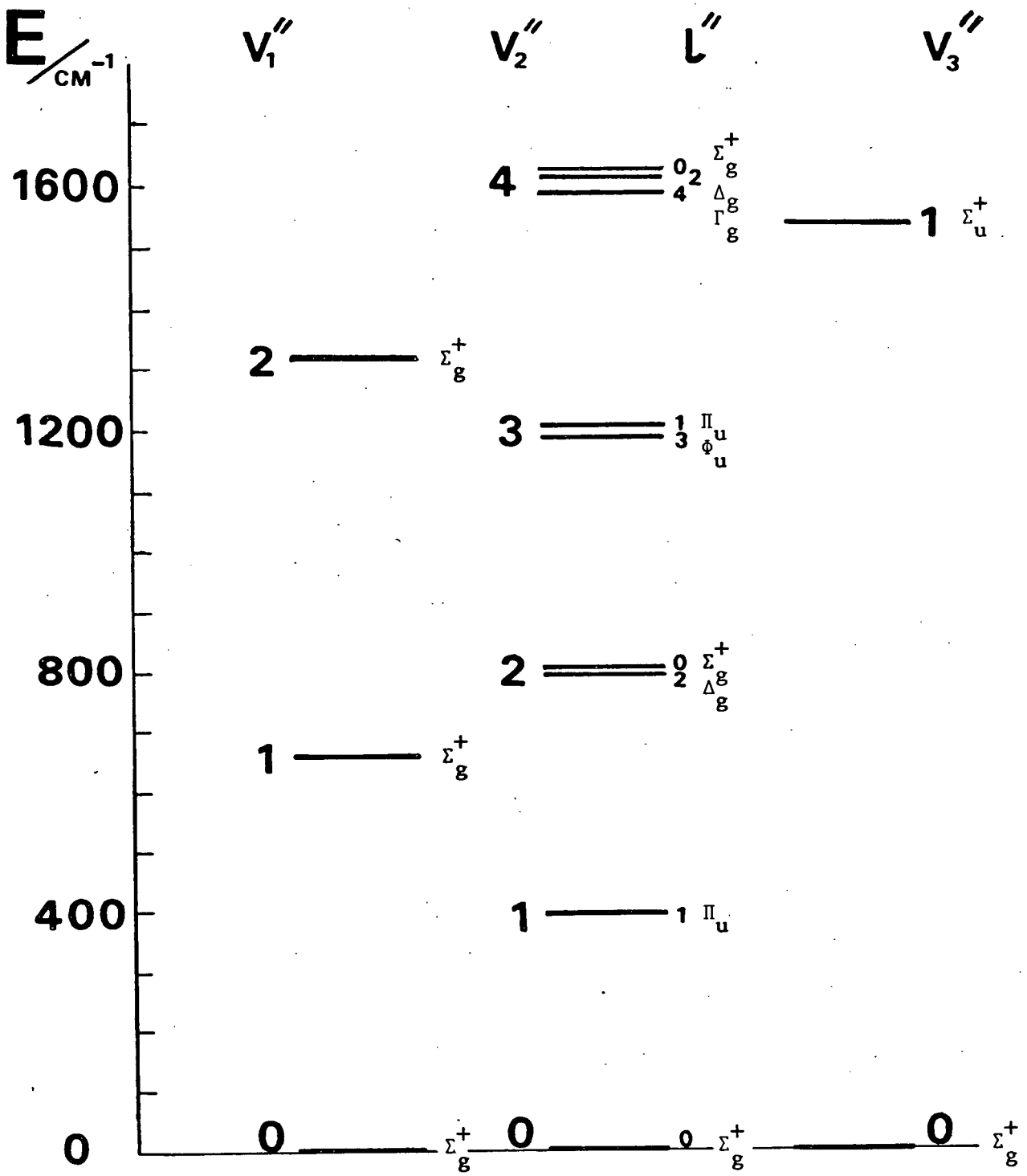

FIG. (2) Fundamental and Lowest-lying Overtone Levels of the $\tilde{X}^1\Sigma_g^+$ Ground State of $^{12}C^{32}S_2$ Referred to the $v_1=v_2=v_3=0$ Level (15,31).

TABLE III

Fundamental and Lowest-lying Overtone Levels (cm^{-1}) of the $\hat{X}^1\Sigma_g^+$ Ground State of $^{12}C^{32}S_2$ Referred to the $v_1 = v_2 = v_3 = 0$ Level (15,31)

$(v_1 v_2^{\ell} v_3)$	Level
$(1\ 0^0\ 0)$	657.98
$(0\ 0^0\ 1)$	1532.35
$(0\ 1^1\ 0)$	395.9
$(0\ 2^2\ 0)$	791.9
$(0\ 2^0\ 0)$	802.6
$(0\ 3^3\ 0)$	1187.8
$(0\ 3^1\ 0)$	1207.2

C. Rotational Energy Level Patterns

The general expression for the rotation-vibration Hamiltonian of a polyatomic molecule in the rigid rotator-harmonic oscillator approximation (32) is

$$\hat{H} = \frac{1}{2} \sum_{\alpha = x,y,z} \frac{(\hat{J}_{\alpha} - \hat{P}_{\alpha})^2}{I_{\alpha}} + \frac{1}{2} \sum_{k} \hat{P}_k^2 + \frac{1}{2} \sum_{k} \lambda_k \hat{Q}_k^2 \qquad (1)$$

The last two terms represent the Normal vibrations of the molecule and have been discussed. The first term refers to the kinetic energy for

nuclear rotation about the three principal inertial axes, as well as the interaction of rotational and internal angular momenta.

We now consider the nuclear rotational kinetic energy. The nuclear rotational angular momentum $\underset{\sim}{R}$ is not quantized: the conserved quantities are $\underset{\sim}{J}$, the total angular momentum, and $\underset{\sim}{P}$, the internal angular momentum, which consists of the vibrational, electron spin and electron orbital angular momenta, i.e.

$$\underset{\sim}{P} = \underset{\sim}{G} + \underset{\sim}{S} + \underset{\sim}{L} . \qquad (2)$$

The nuclear rotational angular momentum is thus obtained by vector subtraction.

$$\underset{\sim}{R} = \underset{\sim}{J} - \underset{\sim}{P} \qquad (3)$$

There is at once a difference between a linear molecule and a non-linear molecule. Since the mass of the linear molecule is concentrated along the axis, I_z is undefined, and $I_x = I_y$. For a non-linear triatomic molecule the three moments of inertia are all different and non-zero, and the planarity condition, $I_x = I_y + I_z$, applies.

We assume that the molecule is in an electronic singlet orbitally non-degenerate state, so that $\underset{\sim}{S}$ and $\underset{\sim}{L}$ may be omitted: the only remaining internal angular momentum arises from vibration. It can be shown (33,34) that the vibrational angular momentum only makes important contributions to the rotational energy levels for a linear molecule, so that the two types of molecular geometries may be considered separately.

i) Linear molecules

Expanding the squares, the K.E. operator for a linear molecule is

$$\hat{T} = \frac{1}{2}\frac{(\hat{J}_x^2 + \hat{J}_y^2)}{I} + \frac{\hat{J}_x\hat{G}_x + \hat{J}_y\hat{G}_y}{I} + \frac{1}{2}\frac{(\hat{G}_x^2 + \hat{G}_y^2)}{I} \qquad (4)$$

The last term (34) has the form of corrections to the anharmonicity terms, and we neglect it. The first term may be re-written

$$\hat{T} = \frac{1}{2I}(\hat{\underset{\sim}{J}}^2 - \hat{J}_z^2) \qquad (5)$$

whose eigenvalues are

$$E = \frac{\hbar^2}{2I}[J(J+1) - \ell^2] \qquad \text{joules} \qquad (6)$$

where the component of $\underset{\sim}{J}$ along the axis of the molecule is the z-component of the vibrational angular momentum, $\ell(\hbar)$. It is customary to use wave number units (cm^{-1}) instead of true energy units (joules), so that we divide both sides by hc:

$$E/hc = \frac{h}{8\pi^2 cI}[J(J+1) - \ell^2] \qquad cm^{-1} \qquad (7)$$

Again, it is customary to abbreviate $h/8\pi^2cI$ by the symbol 'B' (called the rotational constant), giving

$$E/hc = B[J(J+1) - \ell^2] \qquad cm^{-1} \qquad (8)$$

The effects of the second term in (4) are beyond the scope of this thesis, but give rise to the effect called ℓ-type doubling (33)

in degenerate vibrational states where $|\ell| > 0$: the levels of a given J are split by an amount proportional to $B[\frac{B}{\omega} J(J + 1)]^{|\ell|}$ and since in general $B << \omega$, the splitting is largest for $|\ell| = 1$ and decreases rapidly for larger ℓ values. The magnitude of the splitting, expressed by the energy level term $q[J(J + 1)]^{|\ell|}$ may reach a few cm^{-1} units at the highest observable J values. In CS_2 the ℓ-type doubling proportionality constant, q, is only 5.27×10^{-5} cm^{-1} (35).

ii) Non-linear molecules

Energy level expressions for non-linear triatomic molecules cannot be obtained in closed form except for the lowest J values because the molecules belong to the class known as Asymmetric tops, where all three moments of inertia are different. However approximate forms are readily obtained by omitting the off-diagonal matrix elements of the hamiltonian that arise when Symmetric top basis functions are used (the Near-Symmetric top approximation).

The internal angular momentum components can be neglected since their effect is merely to modify the rotational constants of the molecule in a particular vibrational level (33). The hamiltonian for nuclear rotation is then

$$\hat{H} = \frac{\hat{J}_x^2}{2I_x} + \frac{\hat{J}_y^2}{2I_y} + \frac{\hat{J}_z^2}{2I_z} \qquad (9)$$

With the definition of the 'ladder' operators

$$\hat{J}_{\pm} = \hat{J}_x \pm i\,\hat{J}_y$$

this becomes

$$\hat{H} = \frac{1}{2}\left(\frac{1}{2I_x} + \frac{1}{2I_y}\right)\hat{\underset{\sim}{J}}^2 + \left[\frac{1}{2I_z} - \frac{1}{2}\left(\frac{1}{2I_x} + \frac{1}{2I_y}\right)\right]\hat{J}_z^2 +$$

$$+ \frac{1}{4}\left(\frac{1}{2I_x} - \frac{1}{2I_y}\right)\left(\hat{J}_+^2 + \hat{J}_-^2\right) \qquad (10)$$

Converting to cm^{-1} units, and introducing the three rotational constants

$$A = \frac{h}{8\pi^2 c I_z} \qquad B = \frac{h}{8\pi^2 c I_y} \qquad C = \frac{h}{8\pi^2 c I_x} \quad cm^{-1}$$

such that $A > B > C$, we have

$$(\hbar^2/hc)\,\hat{H} = \frac{1}{2}(B + C)\,\hat{\underset{\sim}{J}}^2 + \left[A - \frac{1}{2}(B + C)\right]\hat{J}_z^2 + \frac{1}{4}(C - B)\left(\hat{J}_+^2 + \hat{J}_-^2\right) \qquad (11)$$

Using symmetric top basis functions, $|JK\rangle$, written in molecule-fixed coordinates, the matrix elements of these operators are (36,37)

$$\langle JK|\hat{\underset{\sim}{J}}^2|JK\rangle = J(J + 1)\hbar^2$$

$$\langle JK|\hat{J}_z|JK\rangle = K\hbar \qquad (12)$$

$$\langle J, K \mp 1|\hat{J}_\pm|JK\rangle = \sqrt{J(J + 1) - K(K \mp 1)}\;\hbar$$

The first two terms in the hamiltonian are diagonal, and provided $\frac{1}{4}(C - B)$ is small enough to allow the off-diagonal elements to be neglected, give the energy levels as

$$E/hc = \left[A - \frac{1}{2}(B + C)\right]K^2 + \frac{1}{2}(B + C)\,J(J + 1) \qquad cm^{-1} \qquad (13)$$

The last term in the hamiltonian, which is off-diagonal in K, gives rise to what is called the 'asymmetry doubling' of levels with $K \neq 0$. The asymmetry doubling has the same form as the ℓ-type doubling, being proportional to $[J(J+1)]^K$: however, the proportionality constant is very much larger, so that the asymmetry doubling of an asymmetric top molecule is an order of magnitude greater than the ℓ-type doubling of a linear molecule.

D. Rotational Constants

The three different moments of inertia of a non-linear symmetrical triatomic molecule are calculated in terms of the bond length and the interior angle. The three rotational constants will be evaluated for $^{12}C^{32}S_2$. CS_2 is shown in a non-linear geometry in Fig. 3, where the C-S bond length is ℓ and the S-C-S bond angle is 2ϕ. The orientation of the three principal axes of inertia is defined by the C_{2v} symmetry and their origin by the center of mass condition.

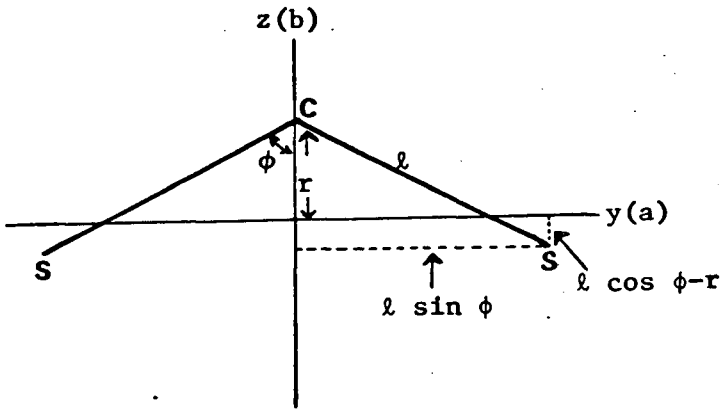

FIG. (3)

The moments of inertia are

$$I_b = 2m_S \ell^2 \sin^2\phi \tag{1}$$

$$I_a = \frac{2m_C m_S}{2m_S + m_C} \ell^2 \cos^2\phi \tag{2}$$

$$I_c = 2m_S\ell^2 \left[1 - \frac{2m_S}{2m_S + m_C} \cos^2\phi\right] \tag{3}$$

where m_C = 12 amu and m_S = 31.97207 amu. With the C-S bond length expressed in Å units, the rotational constants in cm^{-1} units are

$$A = \frac{1.6684}{\ell^2 \cos^2\phi} \tag{4}$$

$$B = \frac{0.26363}{\ell^2 \sin^2\phi} \tag{5}$$

$$C = \frac{0.26363}{\ell^2 [1 - 0.84199 \cos^2\phi]} \tag{6}$$

To calculate the structure of CS_2 (ℓ and 2ϕ) requires knowledge of only two of the three rotational constants because $I_x = I_y + I_z$.

E. Nuclear Spin Statistics

The total eigenfunction of a molecule may be written as a product of the electronic, vibrational, rotational and nuclear spin eigenfunctions.

$$\Psi_{total} = \psi_e \psi_v \psi_r \psi_s. \tag{1}$$

The total eigenfunction can only be symmetric or antisymmetric under the operations of the point group corresponding to exchanging pairs of identical nuclei. If the sum of the individual nuclear angular momenta of the identical nuclei, called $I(\hbar)$, is integral, the total eigenfunction has to be symmetric with respect to exchange of identical nuclei (Bose-Einstein statistics); and, if I is half-integral, the total eigenfunction has to be antisymmetric with respect to exchange of identical nuclei (Fermi-Dirac statistics). In $^{12}C^{32}S_2$, the two identical sulfur nuclei each have zero nuclear spin so that Bose-Einstein statistics apply.

For a linear molecule (29) one need consider only the symmetry properties of the eigenfunctions under inversion of all the particles in the centre of mass, and reflection in any plane passing through the axis. Depending on whether the function does or does not change sign under these operations it is classified as u or g (ungerade or gerade), and - or +, respectively. If the molecule has a centre of symmetry its Hamiltonian is also invariant with respect to an interchange of the coordinates of the nuclei, and a state is classified as 'symmetric' or 'antisymmetric with respect to the nuclei' depending on the behaviour of its eigenfunction with respect to this operation. An interchange of the coordinates of the nuclei is equivalent to a change in the sign of the coordinates of all the particles (electrons and nuclei) followed by a change in sign of the coordinates of the electrons only, i.e. an inversion followed by the reflection described above. Hence it follows that, if the state is gerade and positive or ungerade and negative, it is symmetric with respect to the nuclei.

Since Bose-Einstein statistics apply for the ground vibrational state of CS_2 (where ψ_e, ψ_v and ψ_s are symmetric), the rotational eigenfunction must also be symmetric. Now a rotational eigenfunction $|J\ell>$ is related to the Associated Legendre polynomial characterised by the total and component angular momenta J and ℓ respectively, and its behaviour under the inversion operation is

$$i|J\ell> = (-1)^J|J, -\ell> \qquad (2)$$

Therefore, since $\ell = 0$, only even J functions are symmetric, and are permitted as rotational eigenfunctions. A more detailed consideration (including the effect of the reflection operation) shows that when $|\ell| > 0$, only one member of the ℓ-type doublet for each J value is symmetric and is permitted. The other rotational levels are absent. These patterns are illustrated in Fig. 4.

The nuclear spin statistics of the non-linear CS_2 molecule produce similar rotational patterns. The derivation of the symmetry properties (28,29,38) is more difficult, for it turns out that one must classify the rotational eigenfunctions under the operations of the rotational sub-group C_2: according to the Pauli Principle only those species correlating with the totally symmetric representation of C_2 (i.e. A_1 and A_2 of C_{2v}) are permissible as rotational species. Thus, as shown in Fig. 4, alternate J levels are absent in the K = 0 rotational stacks, and one asymmetry doubling component for each J value of the K > 0 stacks is absent.

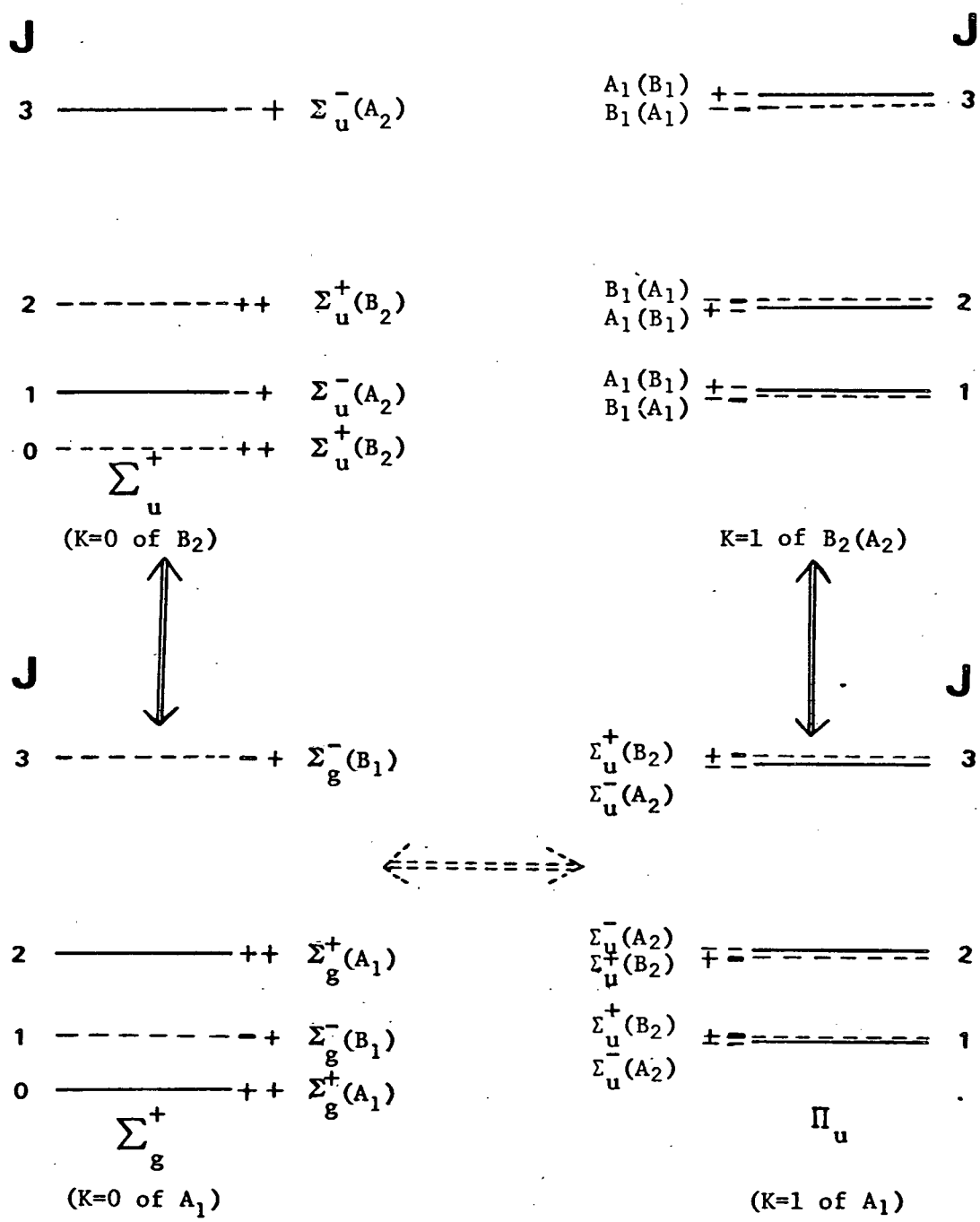

FIG. (4) Asymmetric top species (+−) and rovibronic (over-all) species of the lowest rotational levels of a linear molecule in Σ_g^+, Σ_u^+ and Π_u vibronic states with the corresponding species of a bent molecule in brackets. All rotational levels of B species (dotted lines) are absent in $^{12}C^{32}S_2$ and for K=1 of A_2 dotted and solid lines are exchanged. Parallel and perpendicularly polarized transitions between rotational stacks are shown by solid and dotted arrows, respectively. For all transitions the rovibronic selection rule is $\Sigma_g^+(A_1) \leftrightarrow \Sigma_u^-(A_2)$.

F. Selection Rules

The intensity of an absorption or emission transition for a gaseous molecule is proportional to the square of the transition moment integral

$$R_{evr',evr''} = \langle e'v'r' | \underset{\sim}{\mu}_F | e''v''r'' \rangle \qquad (1)$$

where: the symbols 'evr' refer to the electronic, vibrational, and rotational eigenfunctions of the molecule; the prime and double prime superscripts refer to the upper and lower states; and, $\underset{\sim}{\mu}_F$ is the transition moment operator referred to space fixed coordinates (F) which, for an electronic transition, is the electric dipole moment operator of the molecule. The electric dipole moment operator is a function of internuclear distances, and is therefore usually expanded as a Taylor series in the Normal coordinates of the molecule. The transition moment integral then becomes

$$R_{evr',evr''} = \langle e'v'r' | \underset{\sim}{\mu}_0 + \sum_k \left(\frac{\partial \underset{\sim}{\mu}}{\partial Q_k} \right)_0 Q_k | e''v''r'' \rangle \ , \qquad (2)$$

where the 'F' subscript and the higher terms are omitted.

By neglecting the small influence of the nuclear kinetic energy upon the electronic eigenfunction (Born-Oppenheimer approximation), and the (small) interaction of rotation with other internal motions, we have

$$|evr\rangle = |e\rangle|v\rangle|r\rangle \qquad (3)$$

Thus, equation (2) becomes

$$R_{evr',evr''} = \left\langle r' \middle| \langle e' | \underset{\sim}{\mu}_o | e'' \rangle \middle| r'' \right\rangle \langle v' | v'' \rangle$$

$$+ \delta_{e'e''} \sum_k \left\langle r' \middle| \left(\frac{\partial \underset{\sim}{\mu}}{\partial Q_k} \right)_0 \langle v' | Q_k | v'' \rangle \middle| r'' \right\rangle \tag{4}$$

The second term is the transition moment of a vibrational-rotational (infrared) transition and will not be discussed further. The first term, however, is the transition moment of an electronic or pure rotational (microwave) transition. In a pure rotational transition, e' = e", so that the inner integral is simply the permanent dipole moment of the molecule. In an electronic transition, this integral is the electronic transition moment operator; the other integral in the first term, $\langle v' | v'' \rangle$, is the Franck-Condon vibrational overlap integral.

The components of the electronic transition moment expressed in a molecule-fixed coordinate system (g) are related to the components referred to space-fixed coordinates (F) by the direction cosines, λ_{Fg}.

$$\mu_F = \sum_{g=x,y,z} \lambda_{Fg} \mu_g \tag{5}$$

Using symmetric top eigenfunctions referred to the molecule-fixed coordinates, we have

$$R_{evr'evr''} = \langle v' | v'' \rangle \sum_g \langle J'K' | \lambda_{Fg} \mu_{e'e'',g} | J''K'' \rangle$$

$$= \langle v' | v'' \rangle \sum_g \mu_{e'e'',g} \langle J'K' | \lambda_{Fg} | J''K'' \rangle \tag{6}$$

The determination of rotational line strengths and selection rules is done by calculating the 'direction cosine matrix element', the integral within the sum. The relative intensities of rotational lines in a vibrational band of an electronic transition are given by the square of the line strength (equation (6) with the vibrational overlap integral omitted) summed over the space-fixed components, J_Z and multiplied by the Boltzmann population factor of the lower rotational state. The selection rules on J and K are determined from the non-vanishing direction cosine matrix elements (40) as summarized below for a linear molecule.

Non-zero component of electronic transition moment	Selection Rules
$\mu_{e'e'',z}$ parallel polarization	$\Delta K=K'-K''=0$ $\Delta J=\pm 1$ if $K=0$ $\Delta J=0,\pm 1$ if $K\neq 0$
$\mu_{e'e'',x}$ or $\mu_{e'e'',y}$ perpendicular polarization	$\Delta K=\pm 1$ $\Delta J=0,\pm 1$

The axis labelling must be changed for the non-linear molecule but the selection rules are unaffected.

The projection of J on the axis of a linear molecule is P; the projection of J on the principal axis of least inertia (a axis) of a non-linear molecule is K. A change in geometry of the molecule does not affect the selection rules although the origin of the angular momenta is different in the bent and linear molecules. With parallel-polarization, a $K' = 0 - K'' = 0$ band ($\Sigma - \Sigma$) has a P branch ($\Delta J = -1$) and an R branch ($\Delta J = +1$) with line strengths that increase with J; other parallel bands, $K \neq 0$ (Π-Π, Δ-Δ, etc.) have Q branches ($\Delta J = 0$) that are weak in comparison to the R and P branches and whose line strengths decrease with J. With perpendicular polarization (Σ-Π, Π-Σ, etc.), the P,Q, and R branches are of comparable intensity, with line strengths increasing with J.

The electronic transition vibrational selection rules for a linear molecule are already partially included in the rotational selection rules since P is equivalent to the vibrational angular momentum ℓ of a linear molecule. The only other vibrational selection rule arises from the requirement that the Franck-Condon overlap integral, $\langle v' | v'' \rangle$, be totally symmetric. Thus, any antisymmetric vibration, such as ν_2 (π_u) and ν_3 (σ_u^+) of a linear triatomic molecule must follow the selection rule $\Delta v_k = 0, \pm 2, \pm 4$, etc. since eigenfunctions belonging to even vibrational quantum numbers contain a totally symmetric component. In a non-linear molecule, the doubly degenerate vibration ν_2 becomes a totally symmetric vibration and one of the rotations so that this restriction no longer applies and all values of Δv_2 are allowed.

One further point to note is that the Franck-Condon overlap integral, which determines the extent and intensity distribution of a vibrational progression, depends strongly on the change in geometry of the molecule upon electronic excitation. The vibration predominantly excited is that one which most nearly describes the shape change upon excitation. If the shape change is large enough, the maximum intensity in the vibrational progression may lie well away from the electronic origin band.

IV. ANALYSIS OF THE V AND T SYSTEMS

The low resolution pressure broadened spectrum of CS_2 in the region 2900Å to 3400Å is shown as Fig. 5. At least three electronic transitions are responsible for absorption in this region. The higher vibrational members of the R and S systems lie in the region 3400-3300Å but are very weak ($\varepsilon_{max} \approx 2$ liters/mole cm (41)). The strongest absorption of CS_2 in the near ultraviolet is due to the V system ($\varepsilon_{max} \approx 40$ liters/mole cm (41)). However, it is still a weak system compared to the $^1B_2 \leftarrow {}^1\Sigma_g^+$ system at 2100Å, indicating that it is a 'forbidden' transition. Unlike the R and S systems, which exhibit regular vibrational patterns and simple rotational structure, the V system does not have any readily apparent vibrational progressions, nor is the rotational structure simple. Under high resolution, the rotational structure of the vibrational bands of the V system is dense and irregular with no obvious simple branch-like structure. Without temperature studies, it is not even possible to establish the ground state vibrational numbering of the V bands.

A. Temperature Studies and Polarization of the V System

Part of the complexity of the V system is because bands arising from various vibrational levels of the ground state are present, often with very considerable intensity. To identify these 'hot' bands the spectrum of CS_2 between 2900 and 3500Å was photographed at -78°, 23°, 100° and 200°C: the bands found to be 'hot' are marked with shading on the Cary spectrophotometer tracing (Fig. 5).

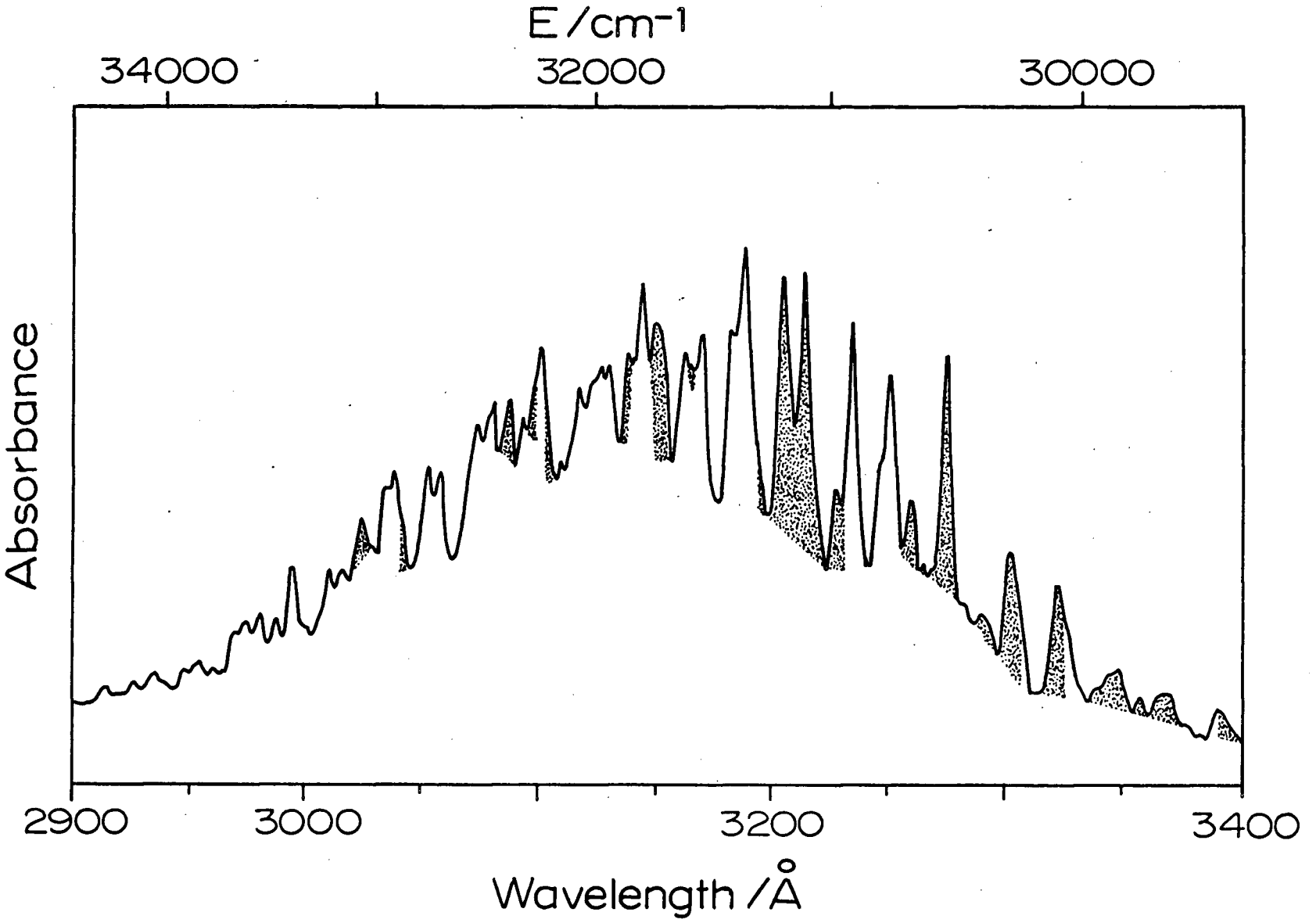

FIG. (5) Room temperature pressure-broadened gas phase absorption spectrum of $^{12}C^{32}S_2$ in the region 2900Å to 3400Å recorded by a Cary 14 spectrophotometer. The shaded areas under the absorption curve indicate absorption from excited vibrational levels of the $\tilde{X}^1\Sigma_g^+$ ground state of CS_2.

A 'hot' band may be recognised by the fact that its intensity increases on raising the temperature of the gas. The intensity of an allowed vibrational band in absorption is proportional to the square of the Franck-Condon overlap integral times the number of molecules in the lower vibrational level, which is given by the Boltzmann distribution

$$\frac{N_v}{N_0} = \exp\ (-E_v hc/RT) \qquad (1)$$

In equation (1), N_v, the number of molecules in level v, at energy E_v relative to the zero-point level, and at temperature T, is given as a fraction of the number, N_0, in the zero-point level. Obviously as the temperature T is increased N_v increases relative to N_0, and N_0 actually decreases because of the number of molecules promoted to the excited vibrational levels. 'Hot' bands are therefore readily identified by comparing spectra taken at different temperatures, and a rough estimate of the energy of the lower level may be obtained by comparing spectra taken at several different temperatures.

As soon as the large number of 'hot' bands in the V system had been recognised, a systematic search was made for ground state vibrational combination differences between bands with common upper states but different lower states. Only the intervals $0\ 2^0\ 0 - 0\ 0^0\ 0$ and $0\ 3^1\ 0 - 0\ 1^1\ 0$ (respectively 802 and 811 cm^{-1}) could be identified, and no intervals corresponding to $1\ 0^0\ 0 - 0\ 0^0\ 0$ (the ground state stretching vibration, 658 cm^{-1}) were found despite considerable effort. As is shown later, the shape change in the V system is almost purely a change in the bond angle on excitation, which is consistent with the observed ground state intervals.

The observed ground state intervals only occur at the long wavelength end of the spectrum, where the 'hot' bands are very intense. However given the identification of the lower states of these bands, together with the known lower state assignments of the R system, it is possible to compare the degree of temperature sensitivity of all the bands of the V system against the known bands, and hence roughly establish the energy of their lower states relative to the zero-point level. It is also possible to make a lower state vibrational quantum number assignment, because, assuming that only the bending vibration is involved, the differences in temperature-sensitivity are sufficiently large to distinguish bands with $v_2'' = 0$, 1 and 2. It is probable that 'sequence bands' in the symmetric stretching vibration, of the type 1v0 - 1v0, may occur on the higher temperature plates, but they do not have such favourable Franck-Condon factors as the 'hot' bands in the bending vibration, and none of them have been recognised.

The observed combination differences also determine that the transition is parallel-polarized. The ground state interval $0\ 2^0\ 0$ - $0\ 0^0\ 0$ occurs between two very strong bands, the 'cold' band at 3236Å (10V in our notation) and the 'hot' band at 3322Å (1V). If the transition was perpendicularly-polarized ($K' - \ell'' = \pm 1$), the presence of the 'cold' band would show that the upper state had $K' = 1$; then the 'hot'

band would be split by the characteristic 10 cm^{-1} separation between the 0 2^0 0 and 0 2^2 0 components of the $v_2'' = 2$ level. However no such splitting (which would be readily observable) appears, so that the transition is parallel-polarized. This deduction is confirmed by the absence of the corresponding splittings in other instances where they would be expected on the basis of perpendicular polarization, and also (see below) by the results of the rotational analysis.

B. Rotational Analysis

The complexity of the V bands makes rotational analysis of most of the bands quite impossible. However two obvious pairs of bands with common upper states (as indicated by the lower state vibrational combination differences described above) were sufficiently unperturbed to invite an attempt at analysis. These are the $K' = 0$ pair at 3236Å and 3322Å, and the $K' = 1$ pair at 3275Å and 3365Å. The 3365Å band has not previously been recognised as belonging to the V system.

Rotational analyses of these bands were possible for three reasons. First, the extremely high resolution attained on our plates (the measured full width at half maximum of an unblended line being <0.05 cm^{-1}) reduced the blending of lines to a minimum. The second factor which helped greatly was the cooling of the gas to -78°C: this

has the effect of reducing the Doppler width of the lines and removing the absorption lines arising from higher rotational levels of the lower states. Finally, a recent high resolution infrared analysis (35) of the bending vibration levels of the ground state has given accurate constants from which it was possible to calculate the data (Appendix I) for the analysis of the electronic spectra.

In order to check the accuracy of the infrared combination differences, an analysis of a simple $\Sigma - \Sigma$ band at 3326Å (Kleman's 17U band) was undertaken. In this band, which was measured from the same plate as the 3322Å band (1V), the rotational combination differences of 18 branch lines deviated by no more than $\pm$ 0.006 cm^{-1} from their calculated values. Hence, the infrared constants give calculated combination differences as least as accurate as the measured relative line positions ($\pm$ 0.01 cm^{-1}).

The well known method of combination differences (42) was used to analyse the bands. If the position of a rotational level above the vibrational origin of the level is called F(J), the rotational level expression for a vibrational level of the ground state (see section III. C(i)) becomes

$$F(J) = T_0 + B[J(J+1) - \ell^2] - D\,J^2(J+1)^2 + \frac{1}{2}(-1)^J qJ(J+1) \qquad (1)$$

where T_0 is the electronic term value, B and D are the rotational and centrifugal distortion constants respectively, and q is the ℓ-type doubling constant. Therefore, the rotational line positions in a parallel band are given by the expressions

$$R(J) = F'(J + 1) - F''(J)$$

$$= \nu_0 + 2B' + (3B' - B'')J + (B' - B'')J^2 \qquad (2)$$

$$P(J) = F'(J - 1) - F''(J)$$

$$= \nu_0 - (B' + B'')J + (B' - B'')J^2 \qquad (3)$$

where ν_0 is the band origin, and the effect of the D and q terms has been neglected.

However complicated the rotational structures of the upper state may be, an analysis is in principle always possible if the R and P branch lines terminating on the same upper level can be identified. Their separation, known as the second combination difference $\Delta_2F''(J)$, is given by

$$\Delta_2F''(J) = F''(J + 1) - F''(J - 1)$$

$$= R(J - 1) - P(J + 1) \qquad (4)$$

In view of the fantastic complexity of the spectrum, we have only attempted to analyse pairs of bands with a common upper level but different lower vibrational levels, because additional combination

differences become available: these are the separation of levels with the same J in the two lower levels, which can of course be accurately calculated from the high resolution infrared data (35). There is a small difference of B with v, resulting from anharmonicity and Coriolis effects, which is sufficient to make a difference of ~ 0.5 cm^{-1} between the vibrational separations of levels with J" = 0 and J" = 40 in the bands of interest. This turned out to be particularly useful because the J dependence of the vibrational combination differences allowed a J assignment (for J > 20) to within ± 2 quanta.

The rotational analysis was carried out by a trial and error search for vibrational and rotational combination differences. To help with the analysis of the 3275Å and 3365Å bands we wrote a computer programme that gave all the possible sets of four lines (an R and a P line from each band) which were in agreement with the ground state combination differences. The four calculated term values were required to agree within 0.04 cm^{-1}. There were of course large numbers of possible sets of lines picked out by the computer, but, by carefully checking every possible set to ensure that the relative intensities of the four lines were roughly the same, we managed to eliminate so many possible sets that, in virtually all cases, only one assignment remained for each rotational line. The rotational assignments are given as Tables IV and V; the computer programme is given as Appendix II.

The rotational analyses show the following. No Q branch is found in any of the four bands. Hence, the two bands of Fig. 6 are $\Sigma - \Sigma$ type, and those of Fig. 7 are $\Pi - \Pi$ type. This result confirms

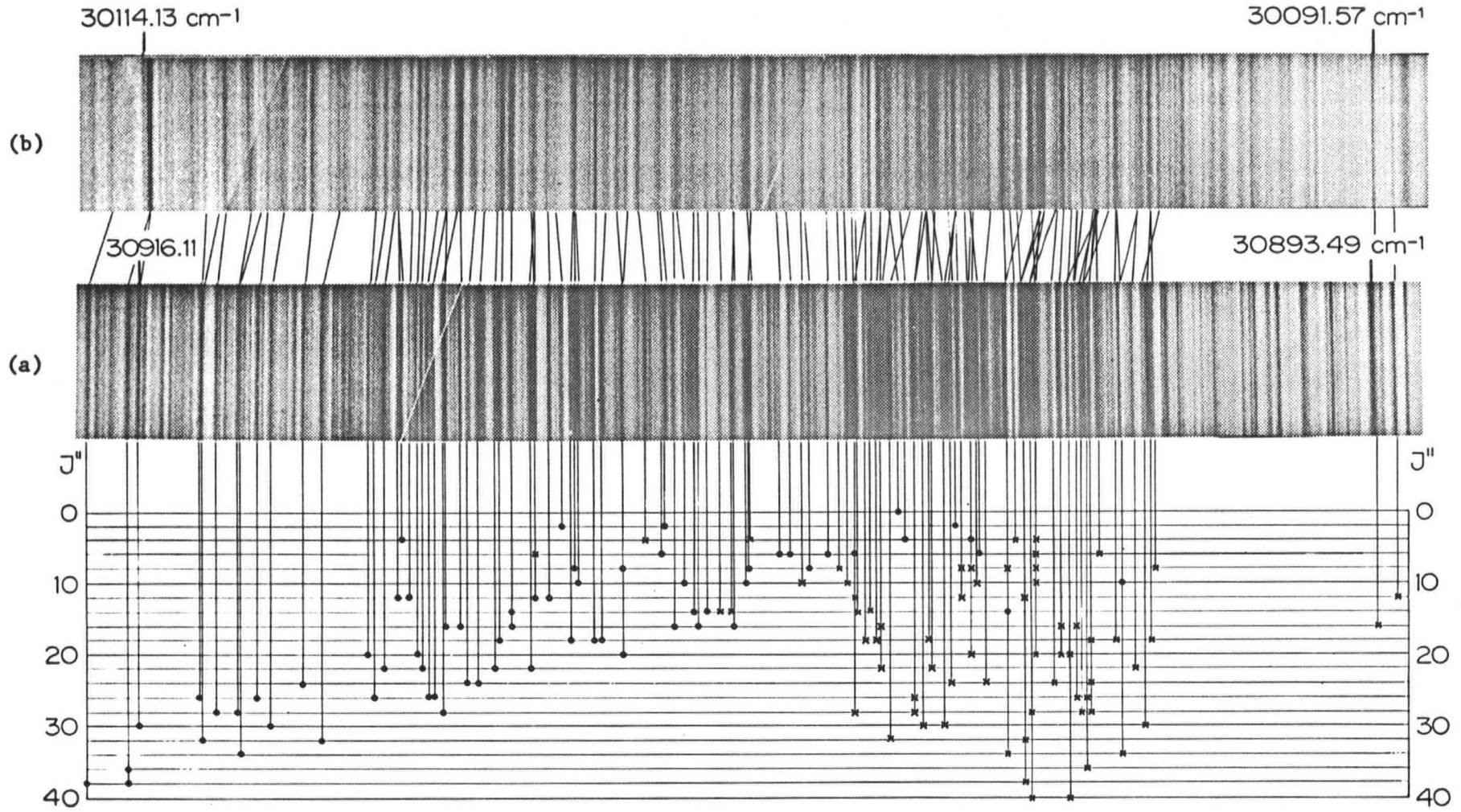

FIG. (6) The (10V) 000, K' = 0 - $00^0 0$ band (a) and the (1V) K' = 0, 000 - $02^0 0$ band (b) of the V system of $^{12}C^{32}S_2$.

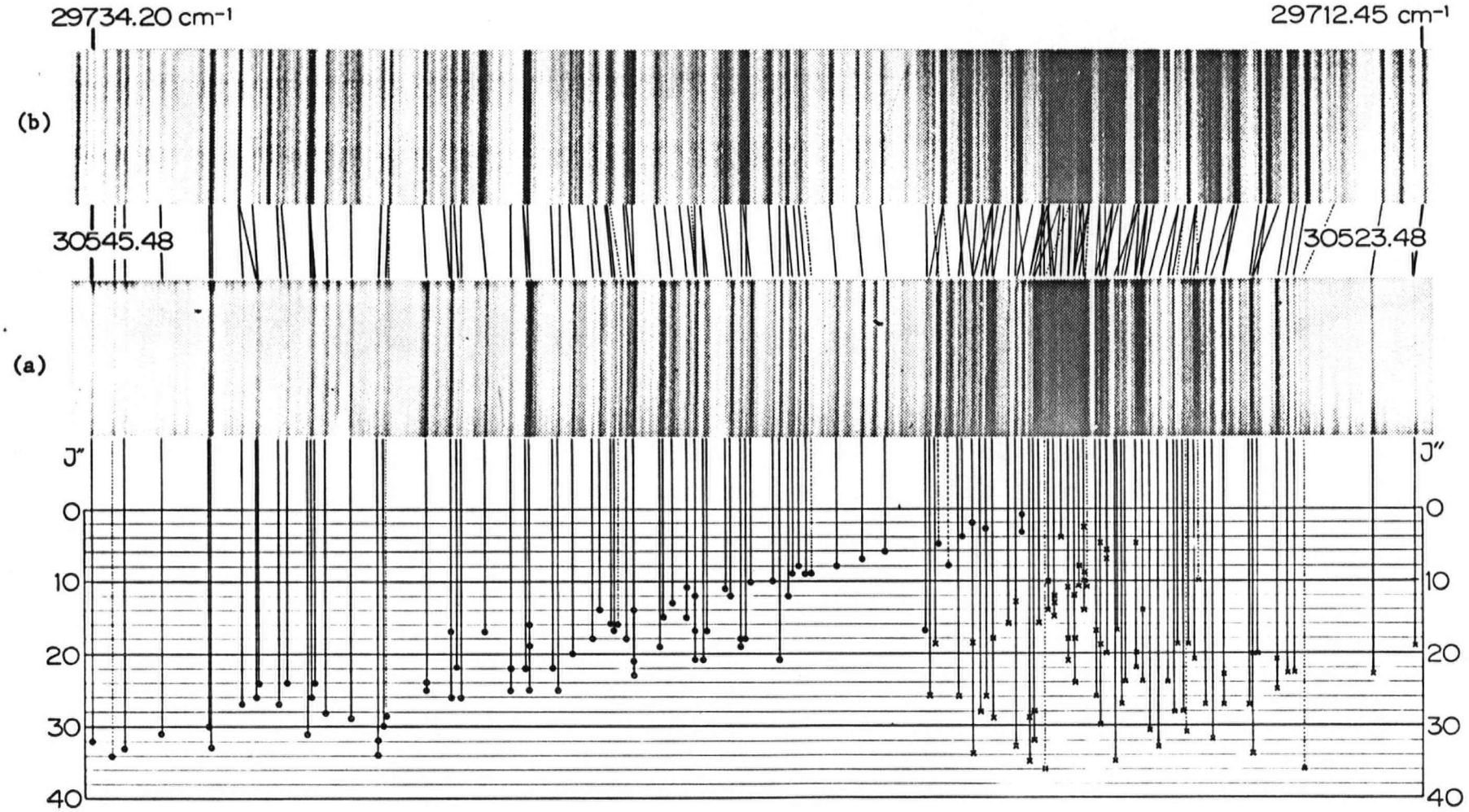

FIG. (7) The (6V) 000, K' = 1 - $01^{1}0$ band (a) and the (3365Å) K' = 1, 000 - $03^{1}0$ band (b) of the V system of $^{12}C^{32}S_2$.

TABLE IV

Rotational Line Assignments of the 3236 Å (10V) and 3322 Å (1V) Bands of $^{12}C\,^{32}S_2$ (cm^{-1}).

	000,K' = 0 - 00°0 (10V)		000,K' = 0 - 02°0 (1V)	
J''	R(J)	P(J+2)	R(J)	P(J+2)
0	30 902.24	30 901.62	30 100.42*	30 099.77
2	901.23*	899.71	099.38	097.83
	901.62	900.09	099.77	098.24
	906.48	904.96	104.63	103.08*
	908.38	906.84	106.54*	105.03
4	900.93	898.53	099.07	096.66
	902.10	899.71	100.27	097.83
	911.29	908.87*	109.40	107.01
6	900.78	897.51	098.93	095.63
	903.02	899.71	101.14	097.83
	903.51	900.26	101.63	098.36
	904.19	900.93	102.37	099.07
	904.39	901.12	102.56	099.25
	906.53*	903.29*	104.66	101.40
8	903.84	899.71	102.01	097.83
	904.96	900.78	103.03	098.93
	907.26	903.14	105.41	101.28
	908.12	903.96	106.26	102.10
10	898.12	893.10	096.24	091.21
	905.01*	899.96*	103.10*	098.09
	906.15	901.12	104.27*	099.25
	908.08	903.02	106.19	101.14
12	908.60	902.71	106.70	100.79
	908.88*	902.97	106.93	101.04
	911.13	905.22*	109.19	103.30
	911.36*	905.46	109.45*	103.57
14	900.26	893.49	098.36	091.57
	905.72	898.95	103.77	097.00*
	905.97	899.20	104.02	097.25
	909.30	902.57	107.37	100.61

TABLE IV (Continued)

16	30 905.24	30 897.58	30 103.30	30 095.63
	905.88	898.24	103.92	096.24
	906.33	898.69	104.39	096.70*
	909.30	901.67*	107.34	099.68
	910.23	902.57	108.28	100.61
	910.48	902.82	108.53*	100.87*
18	907.63	899.08	105.64*	097.10
	907.76*	899.25	105.81	097.25
	908.21	899.71	106.24*	097.68
	909.52	900.93	107.50	098.93
20	907.26	897.88	105.25	095.86*
	911.01	901.62	109.03	099.62
	911.87	902.53*	109.87	100.45
22	908.93	898.69	106.93	096.60*
	909.62	899.40	107.60	097.33
	910.91	900.65	108.90	098.61
	911.59	901.32	109.50	099.25
24	909.88	898.79	107.85	096.66
	910.07	898.95	108.02*	096.88
	913.07	901.93	111.00	099.85
26	910.70	898.69	108.58*	096.53
	910.80	898.79	108.72	096.66*
	911.76	899.81	109.64	097.60
	913.91	901.93	111.80	099.77
	915.00	903.02	112.93	100.89*
28	910.53*	897.58*	108.38*	095.46
	914.26	901.40*	112.14	099.25
	914.66	901.77	112.54	099.62
30	913.66	899.92	111.46*	097.68
	916.11	902.37	113.94	100.10
32	912.73*	898.12	110.50	095.86*
	914.94*	900.28*	112.68	098.01
34	914.23*	898.75*	111.92	096.40
36	916.31	899.95*	113.97*	097.59*
38	916.31	899.08	113.94	096.60*
	917.04	899.80	114.66	097.35*

* measured from high resolution print

TABLE V

Rotational Line Assignments of the 3275 Å (6V) and 3365 Å Bands of $^{12}C^{32}S_2$ (cm^{-1}).

	$000, K' = 1 - 01^1 0$ (6V)		$000, K' = 1 - 03^1 0$ (3365 Å band)	
J''	R(J)	P(J+2)	R(J)	P(J+2)
1	30 529.96	30 528.90	29 719.10	29 717.98
2	30.80	29.30	19.93	18.40
3	30.56	28.63	19.66	17.74
	29.96	28.02	19.10	17.09
4	30.96	28.55	20.06	17.63
5	-	-	-	-
6	32.24	29.00	21.34	18.07
7	32.64	28.90	21.74	17.98
8	33.07	28.93	22.16	17.98
	33.69	29.50	22.75	18.58
9	33.58	29.00	22.67	18.07
	33.79	29.19	22.87	18.26
10	34.12	29.09	23.17	18.12
	34.49	29.43	23.56	18.48
11	34.49	29.00	23.56	18.07
	34.89	29.43	23.97	18.48
	35.55	30.09	24.60	19.10
12	33.85	27.96	22.87	16.97
	34.81	28.93	23.88	17.98
	35.41	29.50	24.48	18.58
13	35.79	29.43	24.85	18.48
14	35.72	28.93	24.76	17.98
	36.43	29.67	25.47	18.67
	36.99	30.22	26.00	19.21
15	35.55	28.35	24.60	17.36
	35.95	28.72	25.00	17.74

TABLE V (Continued)

16	30 536.81	30 529.14	29 725.82	29 718.12
	38.16	30.47	27.14	19.49
17	35.23	27.16	24.24	16.12
	36.75	28.63	25.76	17.63
	38.90	30.80	27.88	19.77
	39.48	31.40	28.46	20.35
18	34.55	26.02	23.51	14.97
	34.66	26.13	23.65	15.11
	36.54	28.02	25.51	16.97
	37.11	28.55	26.09	17.51
19	34.66	25.71	23.65	14.64
	36.00	27.07	25.00	16.02
	38.16	29.19	27.14	18.19
20	37.44	28.02	26.40	16.97
21	34.00	24.17	22.99	13.13
	35.26	25.43	24.24	14.34
	35.41	25.54	24.36	14.51
	36.43	26.58	25.39	15.52
22	37.78	27.51	26.70	16.42
	38.22	27.96	27.14	16.85
	38.50	28.23	27.39	17.09
	39.36	29.09	28.27	17.98
23	36.43	25.71	25.39	14.64
24	39.89	28.72	28.78	17.60
	41.73	30.56	30.64	19.43
	42.19	31.04	31.08	19.93
	42.67	31.52	31.56	20.35
25	37.69	26.11	26.56	14.97
	38.16	26.58	27.09	15.48
	38.50	26.91	27.39	15.79
	39.89	28.27	28.78	17.14
26	39.29	27.27	28.16	16.12
	39.48	27.43	28.34	16.29
	41.78	29.74	30.64	18.58
	42.70	30.68	31.56	19.49
27	42.33	29.84	31.18	18.67
	42.94	30.47	31.80	19.31
28	41.55	28.63	30.38	17.43

TABLE V (Continued)

29	30 541.14	30 527.82	29 529.98	29 516.62
30	40.59	26.79	29.35	15.52
	43.49	29.74	32.27	18.48
31	41.85	27.64	30.64	16.42
	44.28	30.09	33.08	18.82
32	40.75	26.11	29.48	14.80
	45.48	30.80	34.20	19.49
33	43.44	28.40	32.22	17.09
	44.91	29.84	33.66	18.58

TABLE VI(a)

Assigned Rotational Term Values of the (000), $K' = 0$ Level of the $^1B_2(^1\Delta_u)$ V State of $^{12}C^{32}S_2$ (cm^{-1})*.

J'	Term Values						
1	30 902.27						
3	901.88	30 902.28	30 907.13	30 909.04			
5	903.11	904.29	913.46				
7	905.37	907.58	908.09	908.79	30 908.99	30 911.12	
9	911.72	912.80	915.14	916.98			
11	910.13	917.00	918.16	920.07			
13	925.62	925.88	928.13	928.38			
15	923.18	928.62	928.87	932.22			
17	934.91	935.55	936.00	938.97	939.89	940.15	
19	944.92	945.07	945.52	946.79			
21	953.08	956.84	957.70				
23	964.14	964.83	966.12	966.77			
25	975.36	975.54	978.52				
27	987.27	988.33	988.39	990.50	991.60		
29	999.10	31 002.86	31 003.24				
31	31 015.11	017.56					
33	027.93	030.11					
35	044.03						
37	061.61						
39	077.97	078.70					

*Term values are averages from 4 rotational lines with a common upper level.

TABLE VI (b)

Assigned Rotational Term Values of the (000), $K' = 1$ Level of the $^{1}B_2(^{1}\Delta_u)$ V State of $^{12}C^{32}S_2$ (cm^{-1}).†

J'	Term Values			
1	30 926.18			
2	927.46			
3	927.87			
4	929.12			
5	930.64			
6	932.83			
7	934.73			
8	936.93	30 937.52		
9	939.41	939.60		
10	942.12	942.48		
11	944.89	945.30	30 945.95	
12	946.88	947.87	948.46	
13	951.66			
14	955.38	955.93		
15	957.77	958.16	959.00	
16	962.52	963.87		
17	964.65	966.16	968.30	30 968.89
18	967.91	968.04	969.92	970.47
19	972.17	973.53	975.67	
20	979.34			
21	980.49	981.73	981.87	982.90
22	989.09	989.53	989.79	990.66
23	992.74			
24	31 001.47	31 003.31	31 003.78	31 004.24
25	004.70	005.20	005.51	006.89
26	012.04	012.21	014.51	015.44
27	020.91	021.53		
28	026.31			
29	032.20			
30	038.23	041.16		
31	046.24	048.67		
32	052.19	056.89		
33	062.05	063.51		

†Term values (averaged) from the 3275 Å (6V) and 3365 Å bands

beyond doubt the parallel polarization of the V system. The upper state term values are given as Table VI; these term values, suitably scaled by subtraction of $B''_{000} J(J + 1)$, are shown plotted against $J(J + 1)$ in Fig. 8. The two $\Sigma - \Sigma$ bands have only even J" branch lines, as explained in section III.E. The $\Pi - \Pi$ bands, however, have all values of J" present. The observation of several (up to 6) assignments for a single branch line is evidence of the perturbations of the upper state which plagued any previous attempts at rotational analysis of the V bands. The size of the perturbations is illustrated in Fig. 8 by the spread of points for each J' value which is on the order of 5 cm^{-1}. Despite these perturbations there is a definite positive slope of the lines which represents the course of the 'mean' upper state energy levels, indicating that B' > B". The violet degradation of these bands supports such a result. From the slopes and intercepts of the lines are obtained the vibrational band origins and rotational constants:

	Bands	To	B'
(Σ)	3236A, 3322Å	30902.8 ± 0.5 cm^{-1}	0.1129 ± 0.0010
(Π)	3275A, 3365Å	30926.5 ± 0.5	0.1144 ± 0.0010

In the Π vibronic bands, one might expect to find a 'staggering' of even and odd J value branch lines, caused by the Λ or ℓ- doubling of a linear molecule, or, the asymmetry effects in a non-linear molecule as illustrated in Fig. 4. The 'staggering' will appear as a slight

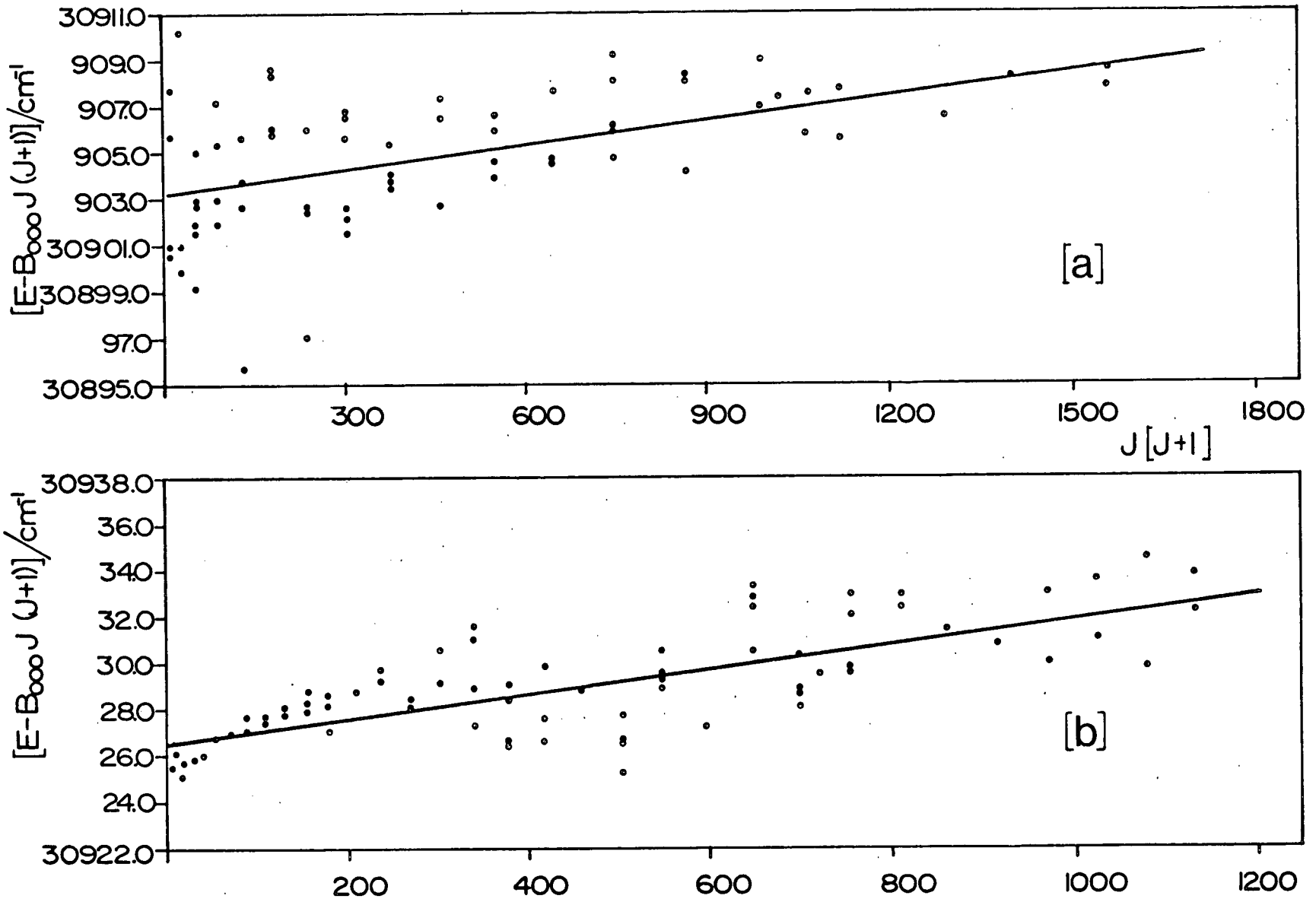

FIG. (8) Rotational Term Values of the 000,K' = 0 Level (a) and the 000,K' = 1 Level (b) of the V State of $^{12}C^{32}S_2$ plotted against J(J+1). The slope of the line - least squares fitted to the average term values - is reduced by subtracting $B''_{000}J(J+1)$ where B''_{000} = 0.1090917 cm^{-1}.

difference in the rotational constant for even and odd J. When the upper state term values are plotted separately for even and odd J, however, the B' values were within one standard deviation of each other. The rotational perturbations in the upper state of the 3275Å and 3365Å bands make the observation of such a 'staggering' impossible. Thus, the rotational analysis indicates that CS_2 in the V state is either linear or not significantly bent. As shown in sections D and F, CS_2 is slightly bent (163°) in the V state so that the calculated asymmetry 'staggering' is much smaller than the standard deviation, ± 0.0010 cm^{-1}, in the rotational constant of the K' = 1 upper state.

A few spurious rotational assignments are inevitable in such a complicated analysis. Nevertheless, at least 90% of the assignments are beyond doubt, which is certainly sufficient to draw conclusions regarding the nature of the upper states involved.

C. Vibrational Pattern of the V State

With the ground state vibrational assignments of the V bands established, the upper state term values were calculated by adding the ground state vibrational energy to the band head positions: these are shown in Fig. 9 and in Table VII. Having determined the parallel polarization, the V levels were grouped according to their values of the projection of the total angular momentum on the molecular a axis, which is called ℓ or K (depending on whether the molecule is linear or bent). The V levels are labelled as Σ, Π, Δ, ... corresponding to K' or ℓ' = 0, 1, 2, ...

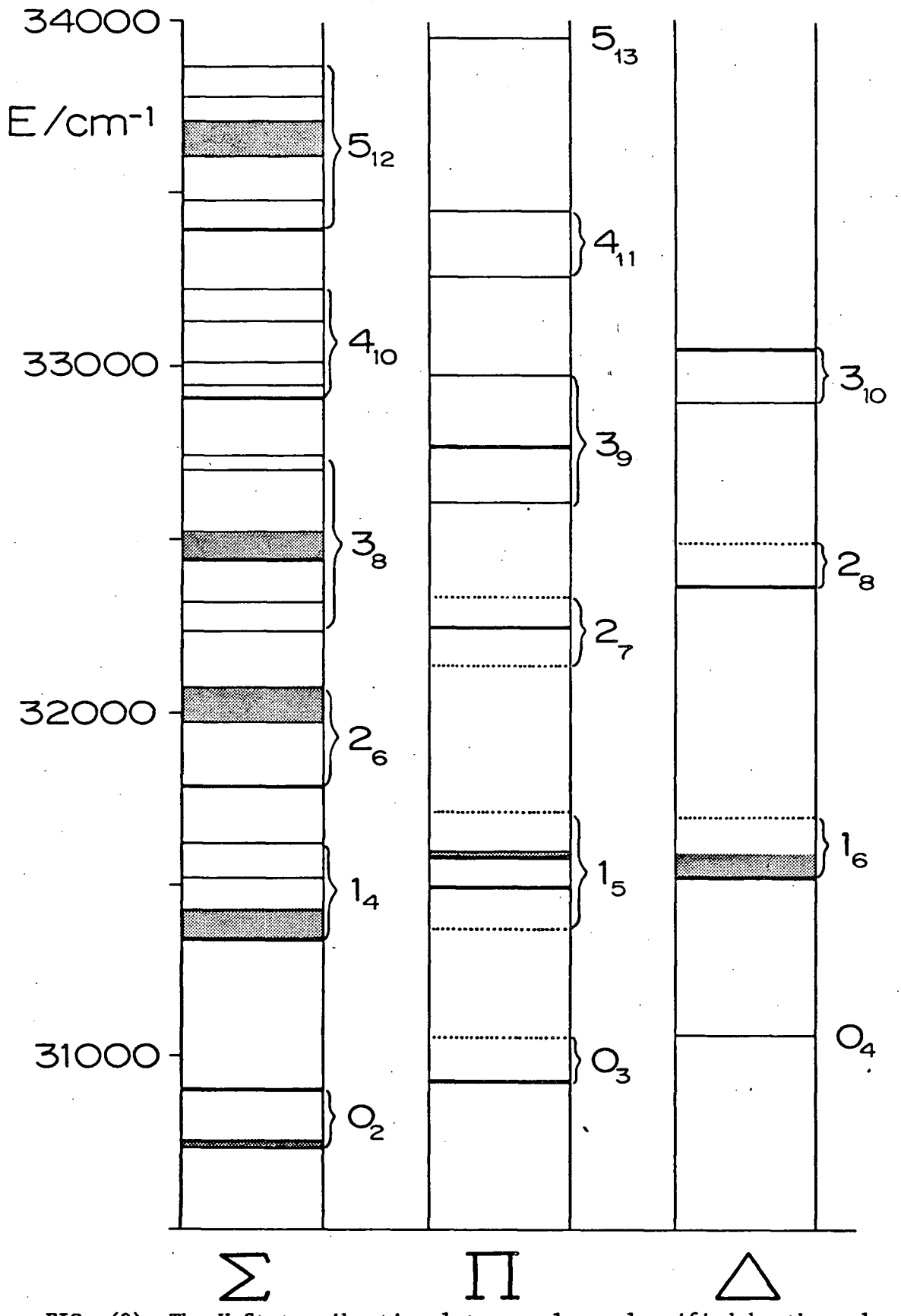

FIG. (9) The V State vibrational term values classified by the value of $\ell'' = 0,1,2$ (Σ,Π,Δ) of the corresponding V bands. Shaded regions indicate bands with no head-like origin; term values of overlapped bands are shown as dotted lines.

TABLE VII

Assigned Term Values of the $\tilde{B}\ ^1B_2(^1\Delta_u) - \tilde{X}^1\Sigma_g^+$ (V) System of $^{12}C^{32}S_2$ (cm^{-1}).

v_2' (bent)	Term Values and v_2' (linear)*							
	Σ		Π		Δ		Φ	
0	(2)	30 756 30 904	(3)	30 757 30 928 (31 057)	(4)	31 066	(5)	30 965 31 178
1	(4)	31 339 31 519 31 625	(5)	(31 372) 31 496 31 594 (31 712)	(6)	31 529 31 703		
2	(6)	31 787 31 974 32 074	(7)	32 140 32 253 32 338	(8)	32 373 32 499		
3	(8)	32 240 32 322 32 445 32 529 32 703 32 747	(9)	32 610 32 772 32 974	(10)	32 906 33 058		

TABLE VII (continued)

	Term Values and v_2' (linear)			
v_2' (bent)	Σ	Π	Δ	Φ
		32 907	(11) 33 269		
		32 945		33 455		
4	(10)	33 010			
		33 133			
		32 218			
		33 389	(13) 33 952		
		33 481			
		33 605			
5	(12)	33 703			
		33 780			
		33 865			

*The v_2'(linear) quantum number is the bracketed number to the left of each group of term values.

The pattern of the Σ levels (corresponding to the 'cold' bands) is very irregular, but can be interpreted as a very perturbed progression of $\sim 580 \pm 30$ cm^{-1}, the same interval as seen in the matrix spectrum at 77°K (22). Since their energies are roughly quadratic in the projection quantum number, the lowest group, with K' or $\ell' = 0$, 1 and 2 can be assigned as the asymmetric top rotational structure of a non-linear molecule (see equation (13) of section III.C) with $A - \frac{1}{2}(B + C) \simeq 33 \pm 5$ cm^{-1}, and, from rotational analysis of Σ and Π levels within these groups (section B), $B \simeq C \simeq 0.11$ cm^{-1}. To be strict, we should use the bent molecule quantum number K' for the projection of the angular momentum along the near-symmetric top a axis, rather than the linear molecule analogue, ℓ', i.e. $K' - \ell'' = 0$. This K-type rotational structure is also seen in the $v_2' = 1$ levels, labelled as 1_4, 1_5 and 1_6 (as explained in section E).

The pattern of the V levels above 32,000 cm^{-1} is quite different, however. The Σ and Δ levels in this region coincide and the Π levels lie halfway between the Σ and Δ levels. Such a pattern (see Fig. 2) is the vibrational energy level pattern of a linear molecule. In other words, the energy level pattern below 32,000 cm^{-1} is characteristic of the K rotational structure of a slightly bent molecule, which, above 32,000 cm^{-1}, becomes the vibrational pattern of a linear molecule with successive excitations of the degenerate bending vibration. The vibrational energy of the non-linear molecule therefore exceeds a potential barrier to linearity at $\sim 31,900 \pm 100$ cm^{-1}. The barrier to

linearity, H, referred to the zero point energy is given by

$$H = (31,900 \pm 100) - E(v_2' = 0) + \frac{1}{2} \nu_2' \qquad cm^{-1}$$

where the lowest-lying V level is taken as the 'mean' position of the $v_2' = 0$ ($K' = 0$) group at 30,830 cm^{-1}. The barrier to linearity is calculated as 1350 ± 150 cm^{-1}. The assignment of the upper state progression to the bending vibration rather than the symmetric stretching frequency (22) is confirmed by the vibrational pattern of the V state. The manifolds of vibrational levels, as grouped in Fig. 9, show the bending vibration and K-type rotational structure expected for a non-linear molecule that overcomes a barrier to linearity on excitation of several quanta of v_2' (43).

The geometry of CS_2 in the lowest vibrational level of the V state can be determined. Knowing the A and B rotational constants, one solves equations (8) and (9) of section III.D for ℓ, the C-S bond length, and 2ϕ, the S-C-S bond angle. The B values obtained from analysis of the 10V and 6V bands are averaged to give $B' = 0.1130 \pm 0.0005$ cm^{-1} so that the geometry of CS_2 can be calculated:

$$r_0(C\text{-}S) = 1.544 \pm 0.006 \text{Å},$$

$$\langle SCS = 163 \pm 2°.$$

The shape change upon excitation of CS_2 from $\tilde{X}^1\Sigma_g^+$ to the V state is mainly a bond angle change and not a bond length change. This is reasonable in light of the observation of extensive 'hot' band structure

in the bending vibration and the absence of the absorption from the ground state symmetric stretching vibrational level. According to the Franck-Condon principle, the calculated geometry of the V state lends further support to the assignment of the V state vibrational progression to the bending vibration, ν_2', because this is the only vibration one expects to see given this shape change.

D. Electronic Species of the V State

The lowest excited electron configuration of CS_2 involves promotion of an electron from the highest occupied orbital, of symmetry π_g, to an antibonding orbital of π_u symmetry. The electronic states of a $(\pi_g)^3(\pi_u^*)^1$ configuration are the singlet and triplet states obtained by group theoretical multiplication, $\pi_u \times \pi_g$. The $\pi \rightarrow \pi^*$ electronic states of CS_2 are therefore

$$^1\Sigma_u^+(^1B_2) \ , \quad ^1\Sigma_u^-(^1A_2) \ , \quad ^1\Delta_u(^1A_2 + {}^1B_2)$$

$$^3\Sigma_u^+(^3B_2) \ , \quad ^3\Sigma_u^-(^3A_2) \ , \quad ^3\Delta_u(^3A_2 + {}^3B_2)$$

where the electronic species of the non-linear molecule are bracketed. As indicated in section III.D, an electronic transition is allowed if the integrand of $\langle e' | \mu_g | e'' \rangle$, where g = x, y or z, is totally symmetric. A parallel-polarized transition involves an oscillating dipole moment parallel to the S-S direction, i.e. of species Σ_u^+ (or B_2). Hence, the V state, where the molecule is non-linear, is a B_2 state.

To decide whether the V state is singlet or triplet (S = 0 or 1) we must consider the results obtained from the magnetic rotation spectrum (16,44). As shown in Appendix III, a magnetic rotation spectrum (m.r.s.) arises from the presence of either an electron orbital or spin angular momentum in one of the two states. Now, the $^1\Sigma_g^+$ ground electronic state has no intrinsic angular momentum so that any observed m.r.s. comes from the upper electronic state.

The R and S systems of CS_2 exhibit a strong m.r.s. (16); the V system, which is considerably stronger in absorption than the R and S systems, has a much weaker, though observable, m.r.s. Since CS_2 in the V state is non-linear so that the orbital angular momentum is essentially quenched, only the spin multiplicity of the V state is in question. Since the R system, known to have a triplet upper state (21), shows a much stronger m.r.s. than the V state, the m.r.s. therefore indicates that the V state is essentially singlet but that perturbations by triplet levels (see section VI) lend some triplet character to the V state, and hence, a weak m.r.s.

Only two $^1B_2$ states can arise from the $(\pi_g)^3\ (\pi_u^*)^1$ configuration, which are the $^1\Sigma_u^+(^1B_2)$ and $^1\Delta_u(^1B_2$ component) states. The $^1\Sigma_u^+(^1B_2)$ state is the upper state of the intense 2100Å system, so that the V state has to be the $^1B_2$ component of the $^1\Delta_u$ state. Thus, the electronic assignment of the V system of CS_2 is $\pi \rightarrow \pi^*\ ^1B_2(^1\Delta_u) - \tilde{X}\ ^1\Sigma_g^+$.

E. Vibronic Correlations in a $^1\Delta$ Electronic State

Figure 10 shows how the vibrational levels of a $^1\Delta_u$ state of a linear molecule correlate with the vibration-rotation levels of the two electronic states which it becomes when the molecule is bent. The left-hand set of vibrational energy levels is that for a $^1\Sigma_g^+$ state; and, the next set is that for a $^1\Delta_u$ state of a linear molecule with small Renner-Teller interaction. Where the Renner-Teller effect is important (sec. V.A.) the only good quantum number is the vibronic angular momentum quantum number $K = |\Lambda + \ell|$, which becomes the rotational quantum number K of the states of a bent molecule. Obeying the 'non-crossing rule' one can therefore draw the correlations between the levels of the linear and bent states directly. These are shown as the tie lines between the second and third sets of levels. The column headed 'vibronic correlation' gives the value $(v_{bent})_{v_{lin}}$ for each K-rotational level.

To illustrate the effect of a potential barrier to linearity upon the energy levels of a molecule in a $^1\Delta_u$ ($^1A_2 + {}^1B_2$) electronic state it is useful to represent the correlations in a different manner. Figure 11 illustrates schematically the course of the K-type rotational levels of the vibrational levels of both the upper and lower component states of the non-linear molecule; the barrier to linearity is arbitrarily assumed to lie at about the $v_{lin} = 7$ level.

The really interesting result of Fig. 11 is the behaviour of the K-type rotational levels of the upper and lower components near the barrier to linearity. If there is no orbital angular momentum,

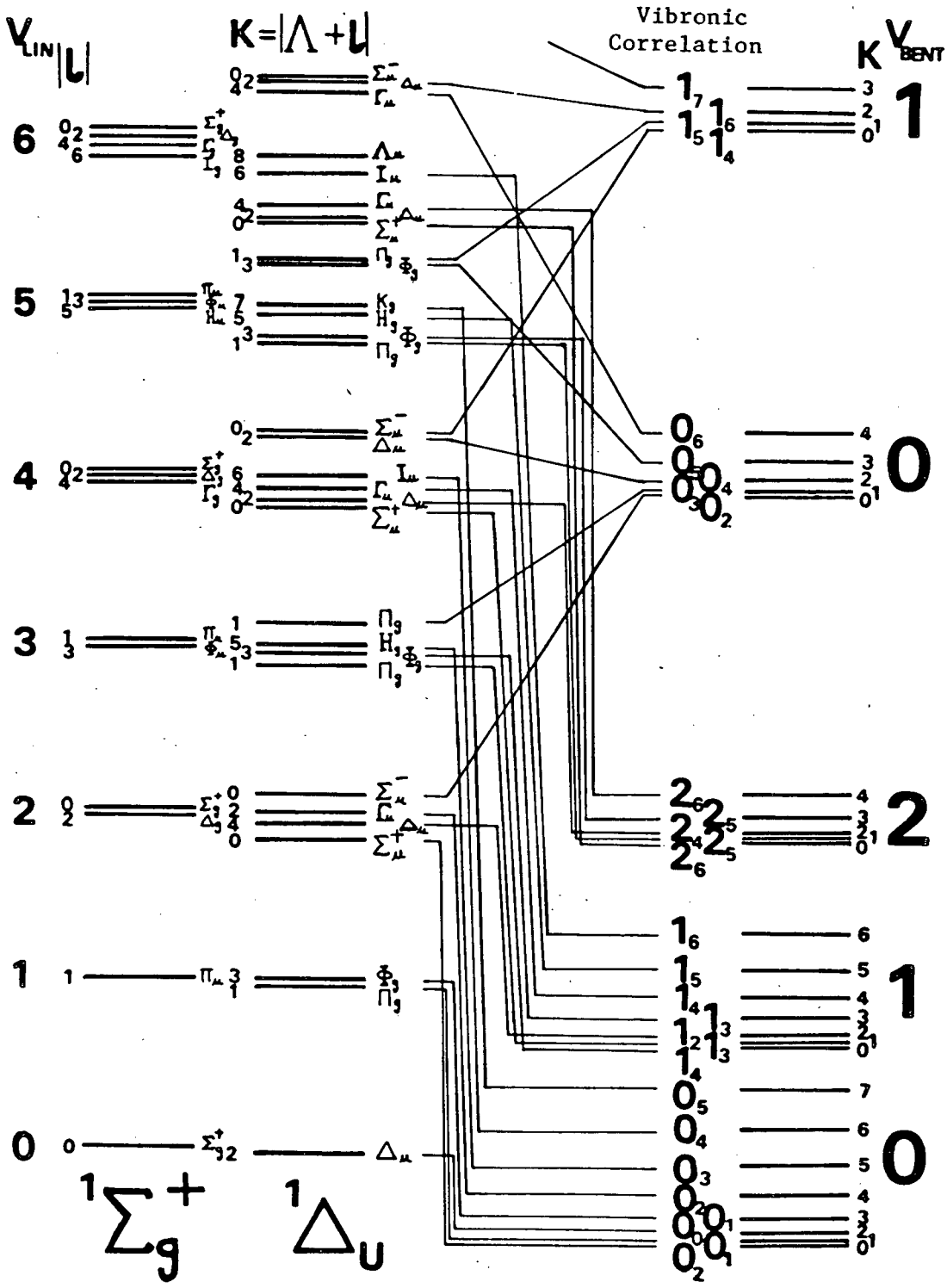

FIG. (10) Correlation of vibronic levels (shown as tie lines) between linear and bent geometries. The bending vibration quantum numbers of a CS_2-type molecule in the linear and bent limits are v_{lin} and v_{bent}, respectively. The levels with the same value of K - the Renner-Teller quantum number of a $^1\Delta_u$ state of a linear molecule and the rotational quantum numbers of a bent molecule - obey a 'non-crossing rule'.

i.e. if $\Lambda = 0$, the symmetric top energy level formula applies (equation (13) of section III.C) and the positions of the K-type rotational levels are quadratic in K. This 'normal' pattern changes near the barrier to linearity to the energy level pattern of a linear molecule. Within the upper component, the value of the A rotational constant (defined here as the energy separation of the K = 1 level above the K = 0 level within a vibrational level) steadily increases as v_{bent} increases, until, near the barrier to linearity, the value of A becomes the linear molecule bending frequency. Within the lower component, however, the behaviour of the value of A is unexpected. Well below the barrier to linearity, the values of A in both components are similar though not equal since the geometries of the molecule in the upper and lower component states are not identical. However, in the higher vibrational members of the lower component state the value of A decreases and actually becomes negative near the barrier to linearity, rapidly approaching the limiting value of the negative of the linear molecule bending frequency. A 'negative rotational constant' is an artifact of the necessary correlation of energy levels within a degenerate electronic state, since a symmetric top A rotational constant cannot be defined for a linear molecule.

This behaviour of the A rotational constant in a Δ state has not been recognized before. As can be seen in Table VIII, in the R state the value of A decreases and becomes negative near the $v_2' = 10$ level (15). Since this effect was not understood by Kleman, he was unable to assign higher vibrational members of the progression. However, we can

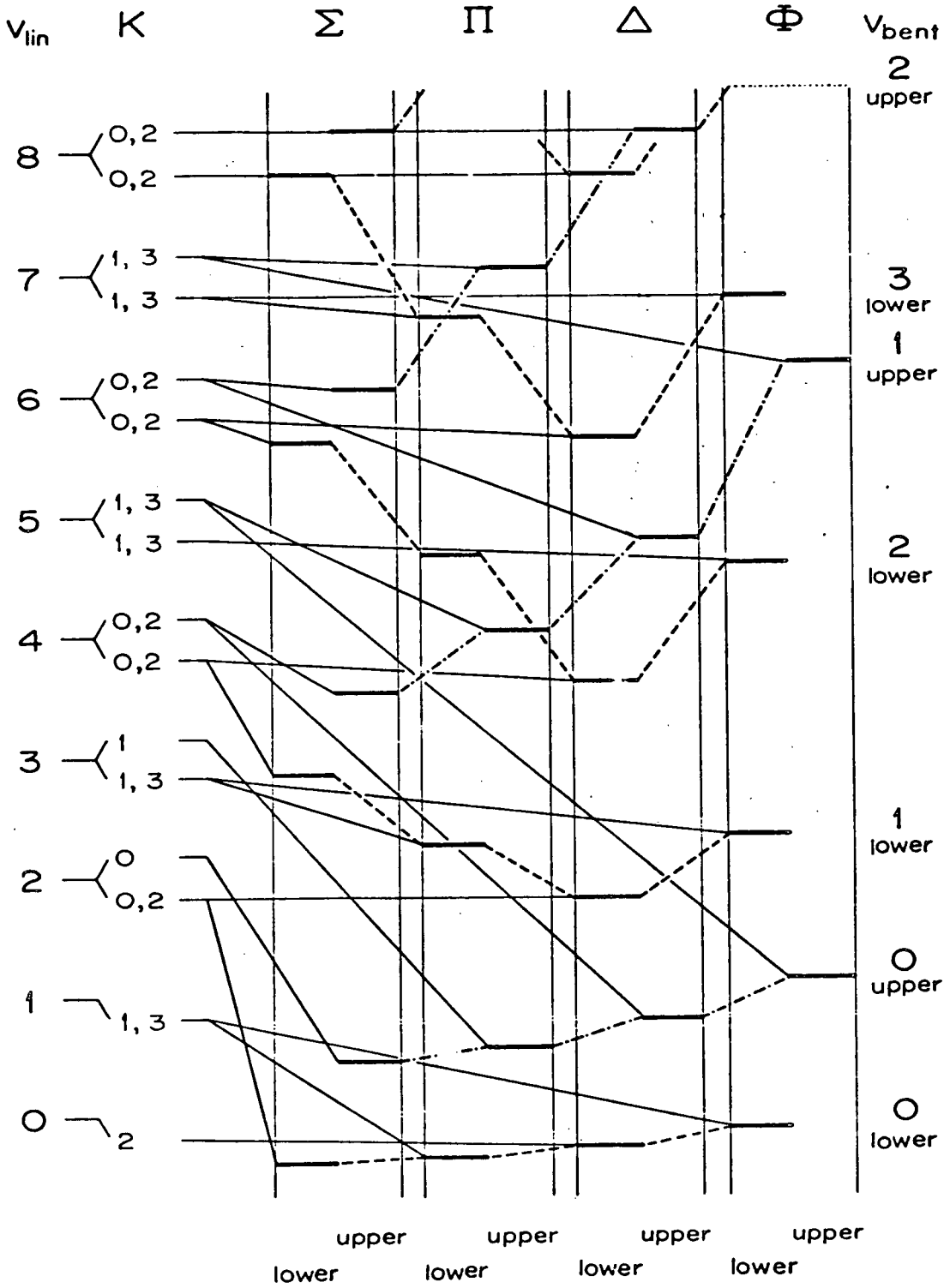

FIG. (11) Behaviour of vibronic levels of the two components of a Δ state with a barrier to linearity at about $v_{lin} = 7$. 'Upper' and 'lower' refer to the two components of a Δ state in the bent molecule limit.

now say that the R state is derived from the lower component of what would be an orbitally degenerate state of the linear molecule. The only possible degenerate $\pi \rightarrow \pi^*$ triplet state is the $^3\Delta_u$ state: Hochstrasser and Wiersma (21), and also Douglas and Milton (19) and Hougen (20), had previously suggested this assignment from Zeeman effect studies, but we can now confirm this from the vibrational structure.

On the other hand, the value of A in the V state increases rapidly near 32,000 cm^{-1}, the barrier to linearity. The V state must be the upper component state. The subscripted correlation labels of the upper component state, as given in Fig. 10, can then be applied to the V state term values in Fig. 9. It should be noted that, above the barrier to linearity, those levels with the same value of the subscripted correlation number (v_{lin}) now coincide, as expected.

TABLE VIII

Term Values of the R^3A_2 ($^3\Delta_u$) State of CS_2*

	$^{12}CS_2$					$^{13}CS_2$				
v_2'	K = 0		K = 1		K = 2	K = 0		K = 1		K = 2
3	27101.1	7.3	27108.4	14.8	27123.2	27100.3	7.1	27107.4	14.0	27121.4
4	27401.9	7.7	27409.6	16.9	27426.5	27395.9	7.3	27403.2	15.3	27418.5
5	27697.3	8.5	27705.8	18.8	27724.6	27685.6	8.6	27694.2	16.9	27711.1
6	27986.4	9.0	27995.4	21.2	28016.6	27970.0	8.2	27978.2	19.5	27997.7
7	28269.8	6.5	28276.3	23.2	28299.6	28249.4	8.1	28257.5	20.7	28278.2
8	28542.8	7.3	28550.1	16.8	28566.9	28523.0	4.2	28527.2	16.3	28543.5
9	28810.0	-2.7	28807.4			28786.4	-7.0	28779.4		
10	29081.0	-37.1	29043.9			29044.0	-38.2	29005.8		

*Values (in cm^{-1}) from B. Kleman, Can. J. Phys. 41, 2034 (1963).

V. THE T STATE

It has been shown that the V state is the upper Renner-Teller component of a $^1\Delta_u$ state. One might therefore expect a weak transition to the lower component, $^1A_2(^1\Delta_u)$ lying to longer wavelengths. We have found such an absorption (which we call the T system, in keeping with Kleman's nomenclature), lying among the higher bands of the R and S systems.

Although a transition from a totally symmetric lower state to a $^1A_2$ electronic state is electric dipole forbidden, a variety of mechanisms can give a non-zero transition moment. Thus, a $^1A_2 - {}^1\Sigma_g^+$ transition is allowed by electric quadrupole and magnetic dipole selection rules. These types of transitions are generally less intense than an electric dipole transition by factors of $\sim 10^5$ and $\sim 10^8$, respectively (45). Moreover, in any polyatomic molecule, most transitions (except the electronic origin band) allowed in these ways can appear more strongly as vibronically allowed electric dipole transitions via Herzberg-Teller mixing.

However, another type of vibronic interaction, the Renner-Teller effect, can cause a transition of the type $^1A_2 - {}^1\Sigma_g^+$ to appear, when the $^1A_2$ state is one component of a degenerate state whose other component does appear in absorption. Such a transition is parallel-polarized, $K' - \ell'' = 0$, and with intensity proportional with K^2, so that only absorption from $\ell'' = 1, 2, 3, \ldots$ levels occurs (as discussed in section A). That is, one expects a transition consisting of 'hot' bands.

In the region 3300Å to 3400Å there are a number of unassigned bands. Only those bands that show no (strong) magnetic rotation spectrum or Zeeman effect can be considered candidates for a singlet electronic system. Numerous 'hot' bands of singlet nature are present in this region and, in fact, two vibrational progressions were found. The T state term values are given in Table IX and a medium resolution photograph of a few of the T bands is presented in Fig. 12. Since the T system is 'hot' only, the Renner-Teller effect is probably causing the transition to appear, as described in the following section.

A. The Renner-Teller Effect in a $^1\Delta_u$ Electronic State

In orbitally degenerate electronic states (Π, Δ, Φ, ...) of linear molecules the vibrational and electron orbital angular momenta are coupled, as first shown by Renner (46) while working with E. Teller. Because of the Renner-Teller effect, the usual Born-Oppenheimer separation of molecular motion into electronic, vibrational, and rotational parts breaks down. The Renner-Teller effect causes the electronic and vibrational wavefunctions to be mixed so that one considers vibronic and rotational motions. The coupling between vibrational and electron orbital angular momenta is described by an effective hamiltonian, derived by Renner

$$\hat{H}_{Renner} = j\,\theta^{2\Lambda}\cos 2\Lambda(\chi-\phi) \qquad (1)$$

where χ is the angle between the radius vector to a 'valence' electron and an arbitrary reference plane, ϕ is the angle between the plane of

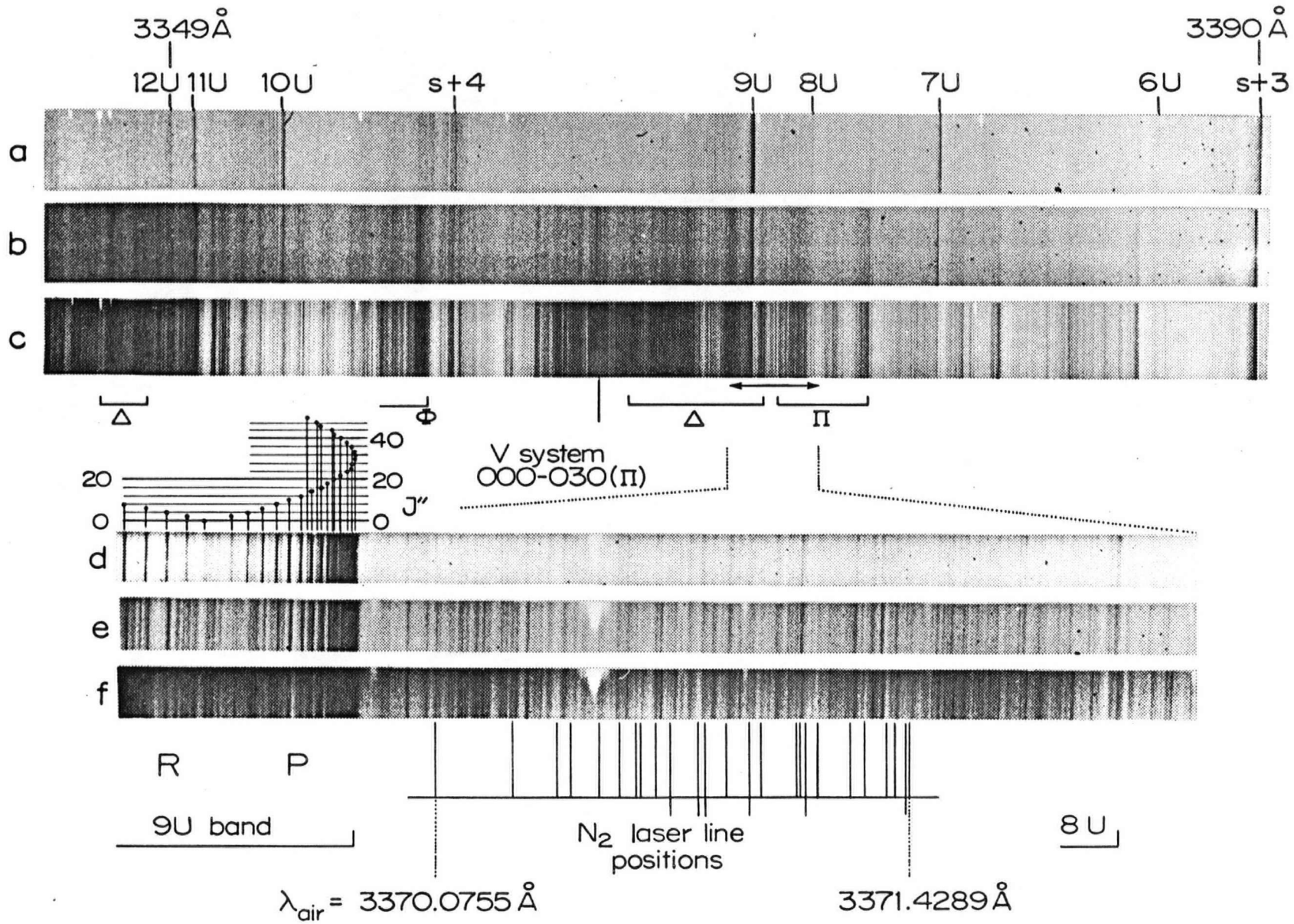

FIG. (12) CS_2 absorption at medium resolution: -78°C (a), 23°C (b) and 100°C (c); and, the 9U region at high resolution: -78°C (d), 23°C (e) and 100°C (f). The (t+2)Δ and tΠ 'hot' bands of the T system are in the region of N_2 laser emission. The rotational analysis of the 'cold' 9U band is shown as a Fortrat-like diagram.

TABLE IX

Assigned Term Values of the T $^1A_2$ ($^1\Delta_u$) State of $^{12}C^{32}S_2$ (cm^{-1})

v_2'	K' = 1	K' = 2	K' = 3
t	30 024	30 031 30 035	30 055
t+1	(30 246)	30 252 30 259	
t+2	30 438 30 444	30 454 30 465	
t+3		30 662 30 670	
t+4		30 844 30 851	

the bent molecule and the same reference plane, θ is the supplement to the instantaneous angle of bend and j is a parameter describing the Renner-Teller interaction.

The Renner-Teller perturbation is best written in exponential form making use of the definition

$$\hat{q}_{\pm} = \theta e^{\pm i(\phi-\chi)} \tag{2}$$

giving

$$\hat{H}_{\text{Renner}} = \frac{1}{2} j \, \theta^{2\Lambda}(e^{2i\Lambda(\chi-\phi)} + e^{-2i(\chi-\phi)})$$

$$= \frac{1}{2} j \, (\hat{q}_{+}^{2\Lambda} + \hat{q}_{-}^{2\Lambda}) \tag{3}$$

In the case of a $^1\Delta_u$ state (Λ=2), the Renner-Teller hamiltonian is

$$\hat{H}_{\text{Renner}} = \frac{1}{2} j \, (\hat{q}_{+}^{4} + \hat{q}_{-}^{4}) \quad ; \tag{4}$$

the Renner-Teller hamiltonian consists of 'ladder' operators mixing electronic and vibrational states according to the rule $\Delta\Lambda = \pm 2$, $\Delta\ell = \mp 2$.

The Renner-Teller term couples the purely electronic wavefunction

$$|\Lambda\rangle = (1/\sqrt{2\pi})e^{i\Lambda\chi} \tag{5}$$

with the doubly degenerate oscillator wavefunction, $|v\ell\rangle$, which contains a vibrational angular momentum term, $(1/\sqrt{2\pi})e^{i\ell\phi}$. The unperturbed 'vibronic' basis function is simply the product of these wavefunctions

$$|\Lambda v\ell\rangle = |\Lambda\rangle|v\ell\rangle \quad . \tag{6}$$

Only the total (vibronic) angular momentum, $\Lambda + \ell$, is conserved by the Renner-Teller interaction. Because of the 'laddering' property of the operator, the matrix elements of the Renner-Teller hamiltonian evaluated in the $|\Lambda v \ell\rangle$ basis functions are entirely off-diagonal. This suggests that symmetrized linear combinations of basis functions, as generated by a Wang transformation, will transfer the interaction mostly to the diagonal matrix elements, and also reduce the size of the off-diagonal elements. Then, second order perturbation theory, rather than exact diagonalization, can be applied.

With the definition $K = |\Lambda + \ell|$, where Λ and ℓ are signed quantities, the 'sum' and 'difference' basis functions are

$$|\Delta^{\pm}\rangle = (1/\sqrt{2})\{|2,v,K-2\rangle \pm |-2,v,K+2\rangle\} \qquad (7)$$

The form of the Renner matrix is illustrated schematically below.

$$\begin{array}{c|cc} & |\Delta^{+}\rangle & |\Delta^{-}\rangle \\ \hline \langle\Delta^{+}| & H_{reord} & H_{FR} \\ \langle\Delta^{-}| & H_{FR} & H_{reord} \end{array}$$

The diagonal sub-matrices contain the 'reordering matrix elements', so designated because these parts of the interaction couple basis functions of the same symmetry. At this stage, one can associate the 'sum' matrix with the upper Renner-Teller component and the 'difference' matrix with the lower component. The reordering matrix elements scramble all the vibrational levels within a component but do not connect the upper and lower component states.

The matrix elements connecting the upper and lower components take the form

$$\frac{1}{2}\, j\, \langle \Delta^{\pm} \mid \hat{q}^4_+ + \hat{q}^4_- \mid \Delta^{\mp} \rangle \tag{8}$$

which we call the 'Fermi resonance matrix elements'. Expressing these matrix elements in the $|\Lambda v \ell\rangle$ basis functions, we have

$$\frac{1}{2}\, j \quad (1/\sqrt{2})\{\langle 2,v,K-2|\mp\langle -2,v,K+2|\}\ |\hat{q}^4_+ + \hat{q}^4_-|\ (1/\sqrt{2})\{|2,v',K-2\rangle \mp |-2,v',K+2\rangle\}$$

$$= \frac{1}{4}\, j\, \{\langle -2,v,K+2|\hat{q}^4_+|2,v',K-2\rangle - \langle 2,v,K-2|\hat{q}^4_-|-2,v',K+2\rangle\} \ . \tag{9}$$

It can be shown that for $K = 0$ the Fermi resonance matrix elements vanish identically. In other words, the Σ^+ and Σ^- vibronic states can be identified with the B_2 (upper) and A_2 (lower) component states, respectively, with no interaction between them. The $K \neq 0$ matrix elements can be calculated easily in harmonic approximation with the definition

$$\hat{q}^4_{\pm} = \hat{x}^4_{\pm}\, e^{\mp 4 i\chi} \tag{10}$$

because matrix elements of the rectilinear displacement operators $\hat{x}_{\pm}$ have been evaluated (47). Matrix multiplication gives the matrix elements of the operator $\hat{x}^4_{\pm}$, and noticing that

$$\langle \pm 2 | e^{\mp 4 i\chi} | \mp 2 \rangle = \frac{1}{2\pi} \int_0^{2\pi} e^{\pm 2 i\chi}\, e^{\mp 4 i\chi}\, e^{\pm 2 i\chi}\, d\chi$$

$$= 1 \ , \tag{11}$$

we have

$$\langle \mp 2, v, K \pm 2 | \hat{q}_{\pm}^4 | \pm 2, v, K \mp 2 \rangle = \frac{3}{2} N \sqrt{(v+K)(v-K)(v+K+2)(v-K+2)}$$

$$\langle \mp 2, v+4, K \pm 2 | \hat{q}_{\pm}^4 | \pm 2, v, K \mp 2 \rangle = \frac{1}{4} N \sqrt{(v \pm K)(v \pm K+2)(v \pm K+4)(v \pm K+6)}$$

$$\langle \mp 2, v+2, K \pm 2 | \hat{q}_{\pm}^4 | \pm 2, v, K \mp 2 \rangle = N \sqrt{(v \mp K+2)(v \pm K)(v \pm K+2)(v \pm K+4)} \qquad (12)$$

$$\langle \mp 2, v-2, K \pm 2 | \hat{q}_{\pm}^4 | \pm 2, v, K \mp 2 \rangle = N \sqrt{(v \mp K+2)(v \mp K)(v \pm K)(v \mp K-2)}$$

$$\langle \mp 2, v-4, K \pm 2 | \hat{q}_{\pm}^4 | \pm 2, v, K \mp 2 \rangle = \frac{1}{4} N \sqrt{(v \mp K+2)(v \mp K)(v \mp K-2)(v \mp K-4)}$$

where N is a normalization factor. The non-vanishing Fermi resonance matrix elements obey the selection rule $\Delta v = \pm 2, \pm 4$.

$$\underline{\Delta v = \pm 2}: \quad H_{FR}^{v+2,v} = N[\sqrt{(v-K+2)(v+K)(v+K+2)(v+K+4)} - \sqrt{(v+K+2)(v-K)(v-K+2)(v-K+4)}]$$

$$= N \sqrt{(v+2)^2-K^2} \; [\sqrt{(v+K+2)^2-2^2} - \sqrt{(v-K+2)^2-2^2}] \qquad (13)$$

For v fairly large, so that $(v+2)^2 >> K^2$ and $(v \pm K+2)^2 >> 4$

$$H_{FR}^{v+2,v} \simeq N(v+2)\,[(v+K+2) - (v-K+2)]$$

$$= 2N(v+2)K \qquad (14)$$

Even for v = 3, K = 1, this approximation is accurate within 7%. Similarly, the $\Delta v = \pm 4$ Fermi resonance matrix elements are also proportional to K, which is a 'good' quantum number.

Applying these results to CS_2, the $^1B_2$ and $^1A_2$ component states of the $\pi \rightarrow \pi^*$ $^1\Delta_u$ state interact with a matrix element proportional to K. The first order wavefunction of the $^1A_2$ state is

$$|{}^1A_2^{(1)},vK\rangle = |{}^1A_2^{(0)},vK\rangle + \sum_{v'} |{}^1B_2^{(0)},v'K\rangle \frac{\langle {}^1A_2^{(0)},vK|H_{FR}^{v,v'}|{}^1B_2^{(0)},v'K\rangle}{E^{(0)}_{{}^1A_2,vK} - E^{(0)}_{{}^1B_2,v'K}} \quad . \quad (15)$$

The vibronic mixing produces a non-zero electric dipole transition moment

$$\langle {}^1A_2^{(1)},vK|\underset{\sim}{\mu}|\tilde{X}{}^1\Sigma_g^+\rangle$$

proportional to K such that the transition takes the parallel polarization of the ${}^1B_2$ (${}^1\Delta_u$) - ${}^1\Sigma_g^+$ transition. Since the intensity of a transition is proportional to the square of the transition moment, the ${}^1A_2({}^1\Delta_u)$ - $\tilde{X}{}^1\Sigma_g^+$ transition has a Renner-Teller induced intensity proportional to K^2.

B. General Features of the T System

It is interesting to note how, at 100°C, the Δ - Δ bands of the T system are stronger than the Π - Π bands. The K^2 intensity term is responsible, since the additional factor of 4 for the Δ - Δ bands (K" = 2) over the Π - Π bands (K" = 1) outweighs the less favourable Boltzmann factor. Only the Renner-Teller effect, as explained above, accounts for the vibronic intensities.

The vibronic Π - Π and Δ - Δ progressions show a vibrational interval of ~ 220 cm^{-1} which must be assigned as the T state bending frequency. Because the T state bending frequency is about half the ground state frequency of 396 cm^{-1}, Π and Δ bands differing by two upper state quanta nearly coincide. The T bands are often doubled and in all cases exhibit rotational structure at least as severely perturbed as that of the V bands so that no rotational analysis has been possible. As in the V state, the term values of the T state show the rotational structure

of a (near) symmetric top molecule. By plotting the average positions of the perturbed levels of the lowest vibrational level against K^2, an A rotational constant of 14.7 ± 1.7 cm^{-1} isobtained. Using the average of the B rotational constants found for the V state, the geometry of CS_2 in the T state was calculated:

$$r(C\text{-}S) = 1.54_4 \pm 0.006\text{Å} \quad \text{(assumed)}$$

$$\langle \hat{SCS} = 155 \pm 2°.$$

In principle, a detailed rotational analysis of a Π - Π band of the T system would allow the magnitude and sign of the asymmetry doubling constant to be determined. The sense of the asymmetry doubling is opposite in the $^1B_2$ and $^1A_2$ component states so that a confirmation of the assignment of the T state as $^1A_2(^1\Delta_u)$ would be provided. Furthermore, without isotopic studies, the absolute vibrational numbering of the T bands cannot be obtained. As yet, the assignment of the T system must not be considered conclusive.

C. N_2 Laser Excited Fluorescence of CS_2 at 3371Å

Brus (49) has reported that CS_2 fluorescence, excited by a pulsed N_2 laser, decays exponentially in the manner expected when the laser initially populates two fluorescing state. Fig. 12 shows the absorption spectrum near the N_2 laser wavelength (3371Å) with the laser lines marked below the high resolution spectra.* The laser lines overlap

*In comparing the CS_2 spectrum with the N_2 laser lines, Brus omitted the vacuum correction to the air wavelengths of the N_2 emission, as given by Park, Rao and Javan (50); the laser lines do not, therefore, fall in the 9U band, as Brus mistakenly thought.

a Π - Π and a Δ - Δ band of the (singlet) T system, and a weak 'cold' band (8U), which is known to be a triplet from its comparatively strong m.r.s. (16). Thus it is possible that Brus' observation of two exponential decays of the laser excited fluorescence of CS_2 may be explained by the fact that the laser lines overlap bands belonging to two electronic transitions, which have singlet and triplet upper states, respectively.

D. The Potential Energy Diagram of the $^1\Delta_u$ State

In a $^1\Delta$ state the potential energy can be written as

$$V^{\pm}(\theta) = V_0 + \frac{1}{2} k\theta^2 + \frac{a}{b+\theta^2} + (\frac{1}{2} \pm \frac{1}{2}) \eta\theta^4 \qquad (1)$$

where + and - refer to the upper ($^1B_2$) and the lower ($^1A_2$) component states, respectively. The first term, V_0, is a constant; the second and third terms represent the potential energy of a bent molecule written as a quadratic term perturbed by a Lorentzian; and the fourth term describes the splitting of the $^1\Delta_u$ state as the linear molecule bends. All the Renner-Teller quartic splitting is included in the upper state potential curve for convenience in calculation.

The four potential energy parameters, k, a, b and η can be calculated from the bond angles, vibrational frequencies and barriers to linearity of the component states. The potential curves must have minima at the upper and lower state equilibrium angles, θ_+ and θ_-, and the second derivatives of equation (1) evaluated at θ_+ and θ_- are

required to reproduce the bending frequencies, $\omega_{\pm}$, i.e.

$$\left.\frac{\partial V^{\pm}(\theta)}{\partial \theta}\right|_{\theta = \theta_{\pm}} = 0 \qquad (2)$$

$$\left.\frac{\partial^2 V^{\pm}(\theta)}{\partial \theta^2}\right|_{\theta = \theta_{\pm}} = \lambda_{\pm} \quad . \qquad (3)$$

The two force constants, $\lambda_{\pm}$, must be calculated for the geometries of CS_2 in the two states.

$$\lambda = (4\pi^2 c/h)\ \{m_s(m_c + 2m_s \sin^2 \tfrac{1}{2}\theta)/2M\}\ \ r_{CS}^2\ \ \omega^2 \qquad (4)$$

Aforementioned uncertainties in the analysis of the T system make the value of θ_- so determined less useful in the determination of the parameters than the barrier to linearity for the upper state,

$$H_+ = V^+(0) - V^+(\theta_+) = \frac{a}{b} - \frac{1}{2}\, k\theta_+^2 - \frac{a}{b+\theta_+^2} - \eta\theta_+^4 \quad . \qquad (5)$$

Four simultaneous equations (obtained by evaluating equations (3), (5) and the '+' component of (2)) were solved numerically with the aid of a computer programme. The potential constants give the potential diagram shown as Fig. 13.

The bond angle in the T state is well predicted by equation (1), as is the barrier to linearity. If the lowest energy T band (see Table IX) belongs to the $v_2' = 0$ level, the T state barrier to linearity is $2000 \pm 100\ cm^{-1}$, bracketing the calculated value of $1960\ cm^{-1}$.

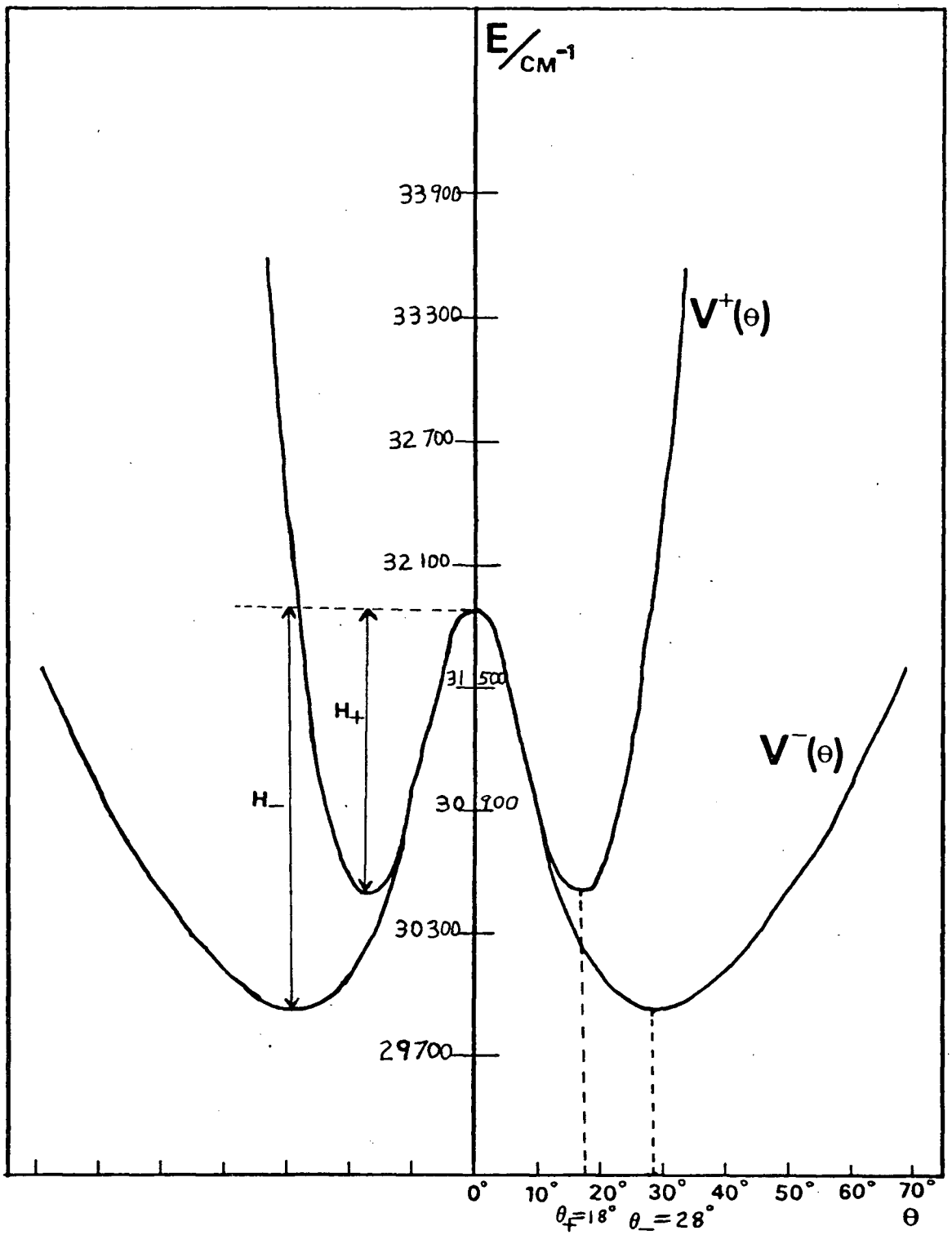

FIG. (13) The potential energy curves of the V and T states (upper and lower curves, respectively).

$$V^{\pm}(\theta) = 29{,}000 + 1730\ \theta^2 + \frac{151.8}{0.0524+\theta^2} + \left(\frac{1}{2} \pm \frac{1}{2}\right) 33900\ \theta^4$$

Using the data $\theta_+ = 18°$, $\omega_+ = 560\ cm^{-1}$, $\omega_- = 220\ cm^{-1}$ and $H_+ = 1350\ cm^{-1}$ gave the above solution with $\theta_- = 28°$, $H_- = 1960\ cm^{-1}$. Cf. the observed values of $\theta_- = 25 \pm 2°$ and tentatively, $H_- = 2000 \pm 100\ cm^{-1}$.

Although the potential energy expression can reproduce the approximate features of the spectrum, it should not be regarded as a confirmation of the vibrational analysis of the V and T systems.

VI. DISCUSSION

Analysis of the electronic absorption spectrum of CS_2 in the region 2900 - 3500Å has shown that the strongest absorption in this region goes to an upper state of $^1B_2$ symmetry where the molecule is bent at equilibrium. A weaker transition at longer wavelengths, which had not been recognized previously, is assigned as going to a $^1A_2$ state, where the $^1B_2$ and $^1A_2$ states are Renner-Teller components of the degenerate $^1\Delta_u$ state ($\pi \rightarrow \pi^*$) of the linear molecule. The molecular structure in the $^1B_2$ state has been determined, and the approximate form of the potential energy curves for the two states has been described.

The observation that the $^1B_2$ component of the $^1\Delta_u$ state lies above the $^1A_2$ component when the molecule is bent gives information about the position of the so-far unobserved $\pi \rightarrow \pi^*$ $^1A_2$ ($^1\Sigma_u^-$) state. The $\pi \rightarrow \pi^*$ $^1B_2$ ($^1\Sigma_u^+$) state is known to lie 15000 cm^{-1} above the $^1\Delta_u$ state (19): by electrostatic interaction it must lower the energy of the $^1B_2$ component. However the $^1A_2$ state interacts similarly with the $^1A_2$ ($^1\Sigma_u^-$) state, and to account for the energy order of the components one can conclude that the $^1A_2$ ($^1\Sigma_u^-$) state lies above the $^1\Delta_u$ state, in contradiction to the considerations of McGlynn et al. (41).

The vibrational and rotational structures of the components of the $^1\Delta_u$ state are very severely perturbed. This is especially so in the V^1B_2 component, where only two upper state levels could be analysed rotationally, and the vibrational structure at the short wavelength end

is chaotic. Evidence from the magnetic rotation spectrum (16) shows that the perturbing states are probably triplet, because the $^1B_2$ component levels below the barrier to linearity (where the orbital angular momentum is quenched) are sensitive to a magnetic field. By classifying the possible $\pi \rightarrow \pi^*$ states according to the case (c) notation one can show that the (strongly) perturbing states are likely to be Kleman's R state, and the $\Omega = 0$ component of the $^3\Sigma_u^-$ state (which is presumably Kleman's S state):-

	$\Omega = 0$	1	2	3
$^1\Sigma_u^+$	B_2 (2100Å bands)			
$^1\Sigma_u^-$	A_2			
$^1\Delta_u$			$A_2(T) + B_2(V)$	
$^3\Sigma_u^-$	$B_2(S)$	$A_1 + B_1$		
$^3\Delta_u$		$A_1 + B_1$	$A_2 + B_2(R)$	$A_1 + B_1$
$^3\Sigma_u^+$	A_2	$A_1 + B_1$		

The singlet and triplet states interact by spin-orbit coupling. In the linear molecule limit this is diagonal in the quantum number Ω, and will allow strong coupling between the $^1\Delta_{2u}$ state and the $^3\Delta_{2u}$ state. In the bent molecule the case (c) spin-electronic states belonging to the same representation are coupled. Thus the $V^1B_2(^1\Delta_u)$ state will be coupled strongly to the $R(^3\Delta_{2u})$ state at all values of the $\hat{SCS}$ bond angle, but more weakly to the $S(^3\Sigma_{0^+u}^-)$ state. The observed perturbations in the $T(^1\Delta_u)$ state are therefore not unexpected, since similar spin-orbit interactions with lower-lying states are possible.

The density of perturbations in the V system is interesting because one is seeing the onset of the spectroscopic manifestation of the process that permits intersystem crossing from the singlet to the triplet manifold of a molecule. The levels we have analysed rotationally belong to the lowest vibrational level of the V state; even so, there are often several assigned upper state levels with the same J value showing that the density of perturbing triplet levels is already considerable. At higher energies the density of lines is much greater and accordingly the density of perturbing triplet levels is obviously also greater. Thus, the spectrum appears to be continuous at low dispersion, although at high resolution it appears as a multitude of overlapping lines so densely packed that their average separations are less than the line width. The diffuse absorption is not a true continuum spectrum because the levels still lie below the ground state dissociation limit (23). A singlet rotational level is perturbed by so many triplet levels in the region of diffuse absorption that the molecule could have a greater probability of being in the triplet manifold than in the singlet manifold.

References

1. E.D. Wilson, Astrophys. J. 69, 34 (1929).
2. F.A. Jenkins, Astrophys. J. 70, 191 (1929).
3. W.W. Watson and A.E. Parker, Phys. Rev. 37, 1013 (1931).
4. L.N. Liebermann, Phys. Rev. 60, 496 (1941).
5. C. Ramasastry, Proc. Natl. Inst. Sci. India A18, 177 (1952).
6. C. Ramasastry, Proc. Natl. Inst. Sci. India A18, 621 (1952).
7. W.C. Price and D.M. Simpson, Proc. Roy. Soc. 165A, 272 (1938).
8. C. Ramasastry and K.R. Rao, Indian J. Phys. 21, 313 (1947).
9. Y. Tanaka, A.S. Jursa, and F.J. LeBlanc, J. Chem. Phys. 32, 1199 (1960).
10. M. Ogawa and H.C. Chang, Can. J. Phys. 48, 2455 (1970).
11. B.P. Stoicheff, Can. J. Phys. 36, 218 (1958).
12. A.H. Guenther, T.A. Wiggins, and D.H. Rank, J. Chem. Phys. 28, 682 (1958).
13. A.D. Walsh, J. Chem. Soc., p. 2266 (1953).
14. A.E. Douglas and I. Zanon, Can. J. Phys. 42, 627 (1964).
15. B. Kleman, Can. J. Phys. 41, 2034 (1963).
16. P. Kusch and F.W. Loomis, Phys. Rev. 55, 850 (1939).
17. A.E. Douglas, Can. J. Phys. 36, 147 (1958).
18. R.S. Mulliken, Can. J. Phys. 36, 10 (1958).
19. A.E. Douglas and E.R.V. Milton, J. Chem. Phys. 41, 357 (1964).
20. J.T. Hougen, J. Chem. Phys. 41, 363 (1964).
21. R.M. Hochstrasser and D.A. Wiersma, J. Chem. Phys. 54, 4165 (1971).
22. L. Bajema, M. Gouterman, and B. Meyer, J. Phys. Chem. 75, 2204 (1971).
23. H. Okabe, J. Chem. Phys. 56, 4381 (1972).
24. J.U. White, J. Opt. Soc. Am. 32, 285 (1942).
25. H.J. Bernstein and G. Herzberg, J. Chem. Phys. 16, 30 (1947).

26. H.M. Crosswhite, Fe-Ne Hollow Cathode Tables, John Hopkins University (1965).

27. R.S. Mulliken, J. Chem. Phys. 23, 1997 (1955).

28. G. Herzberg, Infrared and Raman Spectra of Polyatomic Molecules, Van Nostrand, Princeton, New Jersey, U.S.A. Ch. II 2. (1945).

29. L.D. Landau and E.M. Lifshitz, Quantum Mechanics, 2nd Edition, Pergamon Press and Addison-Wesley Publishing Company, Inc., Reading, Massachusetts, U.S.A. § 101, § 104, § 105, (1965).

30. D. Agar, E.K. Plyler, and E.D. Tidwell, J. Res. Natl. Bur. Stand. 66A, 259 (1962).

31. H.C. Allen, Jr. and P.C. Cross, Molecular Vib-Rotors, John Wiley and Sons, Inc., New York and London, 7 (1963).

32. H. Nielsen, Rev. Mod. Phys. 23, 90 (1951).

33. I.M. Mills, Mol. Phys. 7, 549 (1964).

34. J.T. Hougen, J. Chem. Phys. 36, 519 (1962).

35. D.F. Smith, Jr. and J. Overend, J. Chem. Phys. 54, 3632 (1971).

36. E.U. Condon and G.H. Shortely, The Theory of Atomic Spectra, The University Press, Cambridge, Ch. III (1963).

37. J.H. Van Vleck, Rev. Mod. Phys. 23, 213 (1951).

38. G. Herzberg, Electronic Spectra of Polyatomic Molecules, Van Nostrand, Princeton, New Jersey, U.S.A. 109-114, 223 (1966).

39. J.T. Hougen, Nat. Bur. Stand. (U.S.) Monogr. 115, Ch. 3 (1970).

40. H.C. Allen, Jr. and P.C. Cross, Molecular Vib-Rotors, John Wiley and Sons, Inc., New York and London, 102 (1963).

41. J.W. Rabelais, J.M. McDonald, V. Scher and S.P. McGlynn, Chem. Rev. 71, 73 (1971).

42. G. Herzberg, Infrared and Raman Spectra of Polyatomic Molecules, Van Nostrand, Princeton, New Jersey, U.S.A. 390 (1945).

43. R.N. Dixon, Trans. Faraday Soc. 60, 1363 (1964).

44. W.H. Eberhardt, private communication.

45. G. Herzberg, Electronic Spectra of Polyatomic Molecules, Van Nostrand, Princeton, New Jersey, U.S.A. 134-136, 222, 265-271 (1966).

46. E. Renner, Z. Phys. 92, 172 (1934).

47. W. Moffit and A.D. Liehr, Phys. Rev. 106, 1195 (1957).

48. A.J. Merer and D.N. Travis, Canad. J. Phys. 44, 353 (1966).

49. L.E. Brus, Chem. Phys. Letters 12, 116 (1971).

50. J.H. Parks, D.R. Rao and A. Javan, Appl. Phys. 13, 142 (1968).

51. T. Carroll, Phys. Rev. 52, 822 (1937).

52. W.H. Eberhardt and H. Renner, J. Mol. Spec. 6, 483 (1961).

APPENDIX I

Vibrational and Rotational Combination Differences of the $\tilde{X}^1\Sigma_g^+$ Ground Electronic State of $^{12}C^{32}S_2$

The rotational energy formulae of CS_2 in its ground electronic state used were

$$F(J) = \nu_0 + B_v[J(J+1) - \ell^2] - D_v J^2(J+1)^2 + \frac{1}{2}(-1)^J qJ(J+1) \quad (1)$$

$$\Delta_2 F_v(J) = F_v(J+1) - F_v(J-1) \quad (2)$$

$$\Delta_2 G(J) = F_{v'}(J) - F_{v''}(J) \quad (3)$$

The constants used (35) are summarized below in cm^{-1} units.

Level	ν_0	B_v	$D_v \times 10^8$	$q \times 10^5$
$0\ 0^0\ 0$	0	0.1090917	0.993	0
$0\ 2^0\ 0$	801.849	0.1094604	0.810	0
$0\ 1^1\ 0$	396.092	0.1093146	0.953	5.27
$0\ 3^1\ 0$	1206.980	0.1096572	1.49	8.62

The values of equations (1 - 3) were calculated with the aid of a computer programme and are given here.

J	(0 0^0 0) Level		(0 2^0 0) Level		$\Delta_2G(J)$ =
	$F_0(J)$	$\Delta_2F_0(J-1)$	$F_2(J)$	$\Delta_2F_2(J-1)$	$F_2(J) - F_0(J)$
0	0	-	801.849	-	801.849
2	0.655	0.655	802.506	0.657	1.851
4	2.182	1.527	804.038	1.532	1.856
6	4.582	2.400	806.446	2.408	1.864
8	7.855	3.273	809.730	3.284	1.876
10	12.000	4.145	813.890	4.159	1.890
12	17.018	5.018	818.925	5.035	1.907
14	22.909	5.891	824.835	5.911	1.927
16	29.672	6.763	831.622	6.786	1.949
18	37.308	7.636	839.284	7.662	1.975
20	45.817	8.509	847.821	8.537	2.004
22	55.198	9.381	857.234	9.413	2.036
24	65.451	10.254	867.522	10.288	2.071
26	76.577	11.126	878.686	11.164	2.109
28	88.576	11.998	890.726	12.039	2.150
30	101.447	12.871	903.640	12.915	2.193
32	115.190	13.743	917.430	13.790	2.240
34	129.805	14.615	932.095	14.665	2.290
36	145.293	15.487	947.636	15.540	2.343
38	161.652	16.360	964.052	16.416	2.399
40	178.884	17.232	981.342	17.291	2.459

	(0 1^1 0) Level		(0 3^1 0) Level		
J	$F_1(J)$	$\Delta_2F_1(J)$	$F_3(J)$	$\Delta_2F_3(J)$	$\Delta_2G(J)$
1	396.201	-	1207.090	-	810.888
2	96.639	1.093	07.529	1.096	0.890
3	97.294	1.531	08.186	1.536	0.892
4	98.170	1.967	09.064	1.973	0.895
5	99.261	2.405	10.159	2.413	0.897
6	400.575	2.841	11.478	2.850	0.903
7	02.103	3.280	13.009	3.291	0.906
8	03.855	3.716	14.769	3.727	0.914
9	05.819	4.155	16.735	4.169	0.917
10	08.010	4.590	18.937	4.604	0.927
11	10.409	5.030	21.339	5.046	0.931
12	13.040	5.464	23.983	5.480	0.944
13	15.873	5.904	26.820	5.924	0.947
14	18.944	6.338	29.907	6.357	0.963
15	22.211	6.779	33.177	6.801	0.966
16	25.723	7.213	36.708	7.234	0.985
17	29.424	7.653	40.411	7.678	10.987
18	33.376	8.087	44.386	8.111	811.010
19	37.511	8.528	48.522	8.556	1.011
20	41.904	8.961	52.942	8.987	1.038
21	46.472	9.403	57.509	9.433	1.037
22	51.307	9.835	62.375	9.864	1.068

J	$F_1(J)$	$\Delta_2F_1(J)$	$F_3(J)$	$\Delta_2F_3(J)$	$\Delta_2G(J)$
23	456.307	10.277	1267.373	10.310	811.066
24	61.584	10.709	72.685	10.740	1.101
25	67.016	11.152	78.113	11.187	1.097
26	72.735	11.583	83.873	11.617	1.137
27	78.599	12.026	89.730	12.065	1.131
28	84.761	12.457	95.937	12.493	1.176
29	91.056	12.900	1302.223	12.942	1.167
30	97.662	13.331	08.879	13.370	1.217
31	504.387	13.775	15.593	13.819	1.206
32	11.436	14.205	22.697	14.246	1.261
33	18.592	14.649	29.839	14.695	1.247
34	26.085	15.079	37.393	15.122	1.308
35	33.671	15.523	44.960	15.572	1.290
36	41.608	15.952	52.965	15.998	1.357
37	49.623	16.397	60.958	16.449	1.335
38	58.005	16.826	69.413	16.874	1.408
39	66.449	17.271	77.832	17.235	1.383
40	75.276	17.700	86.739	17.750	1.463

APPENDIX II

CS2 COMBINATION DIFFERENCE PROGRAMME

```
C     LINES OF TWO BANDS WITH COMMON UPPER STATES ARE
C     STORED IN 'V(NI)' AND 'HV(NJ)'.
C     'PREC' IS THE REQUIRED PRECISION(CM-1) OF THE FOUR
C     CALCULATED TERM VALUES GENERATED BY THE R AND P
C     BRANCH ASSIGNMENTS FROM EACH BAND.
C     COMBINATION DIFFERENCES OF CS2 LOWER LEVELS ARE
C     STORED IN ARRAY 'P'. THE CONSTANTS SHOWN ARE FOR
C     THE V2=1,L=1 AND V2=3,L=1 LEVELS.

      DIMENSION P(37,5),V(250),HV(250),SM(10),WR(4,6)
      DO 1 J=1,37
      X=FLOAT(J*J+J)
      P(J,1)=-4.017+(0.1092883-0.0000000953*X)*X
      P(J,2)=6.870+(0.1096141-0.0000000149*X)*X
      IF(MOD(J,2).NE.0) GO TO 22
      P(J,1)=P(J,1)+0.0000527*X
      P(J,2)=P(J,2)+0.0000862*X
   22 P(J,3)=P(J,2)-P(J,1)
    1 CONTINUE
      DO 20 J=2,36
      P(J,4)=P(J+1,1)-P(J-1,1)
   20 P(J,5)=P(J+1,2)-P(J-1,1)
      READ(5,100) NI,NJ,PREC
  100 FORMAT(2I4,F5.3)
      READ(5,101) (V(K),K=1,NI)
      READ(5,101) (HV(K),K=1,NJ)
  101 FORMAT(16F5.3)
      ZL=P(1,3)-PREC
      ZU=P(36,3)+PREC
      LZ=1
      QZ=1.3*PREC
      DO 2 N=2,NI
      Z=V(N)
      WRITE(6,49) Z
   49 FORMAT(/' LINE',F10.3)
      KK=0
      IF((Z-HV(LZ)).LT.ZL) GO TO 2
    4 IF((Z-HV(LZ)).LT.ZU) GO TO 5
    3 LZ=LZ+1
      IF(LZ.GT.NJ) GO TO 2
      GO TO 4
    5 I=LZ
    7 KK=KK+1
      SM(KK)=HV(I)
      I=I+1
      IF(I.GT.NJ) GO TO 6
      IF((Z-HV(I)).GT.ZL) GO TO 7
    6 KN=N-1
      LN=LZ-1
      DO 8 J=1,35
   10 ZA=P(J,3)
      KL=0
      KR=0
```

```
      KS=0
      DO 9 I=1,KK
      IF(ABS(Z-SM(I)-ZA).GT.PREC) GO TO 9
      KL=KL+1
      WR(KL,1)=SM(I)
    9 CONTINUE
      IF(KL.EQ.0) GO TO 8
      I=KN
      ZA=P(J+1,4)
   11 IF(I.EQ.0) GO TO 13
      IF((Z-V(I)+PREC).LT.ZA) GO TO 12
      IF(ABS(Z-V(I)-ZA).GT.PREC) GO TO 13
      KN=I
      KR=KR+1
      WR(KR,2)=V(I)
   12 I=I-1
      GO TO 11
   13 IF(KR.EQ.0) GO TO 8
      I=LN
      ZA=P(J+1,5)
   14 IF(I.EQ.0) GO TO 16
      IF((Z-HV(I)+PREC).LT.ZA) GO TO 15
      IF(ABS(Z-HV(I)-ZA).GT.PREC) GO TO 16
      LN=I
      KS=KS+1
      WR(KS,3)=HV(I)
   15 I=I-1
      GO TO 14
   16 IF(KS.EQ.0) GO TO 8
      T=Z+P(J,1)
      DO 17 I=1,KL
   17 WR(I,4)=WR(I,1)+P(J,2)
      DO 18 I=1,KR
   18 WR(I,5)=WR(I,2)+P(J+2,1)
      DO 19 I=1,KS
   19 WR(I,6)=WR(I,3)+P(J+2,2)
      IF((KL+KR+KS).NE.3) GO TO 21
      IF((AMAX1(WR(1,4),WR(1,5),WR(1,6))-AMIN1(WR(1,4),WR(1,5),WR(1,6)))
     1.GT.QZ) GO TO 8
   21 WRITE(6,50)J,T,(WR(I,1),WR(I,4),I=1,KL)
   50 FORMAT(' R(',I2,')',F10.3,45X4(F7.3,F8.3))
      WRITE(6,51)(WR(I,2),WR(I,5),I=1,KR)
   51 FORMAT(1X4(F7.3,F8.3))
      WRITE(6,52)(WR(I,3),WR(I,6),I=1,KS)
   52 FORMAT('+',60X4(F7.3,F8.3))
    8 CONTINUE
    2 CONTINUE
      STOP
      END
```

APPENDIX III*

The magnetic rotation spectrum (m.r.s.) of a gas is a spectrum of the light transmitted by a gas placed between crossed polarizers and with a magnetic field acting upon the gas in a direction parallel to the propagation of the light. The rotation of the plane of polarization is proportional to the product of the magnetic field strength times the path length times the density of the gas.

The magnetic field removes the spatial degeneracy of the total angular momentum, J of the molecule. Hence, J and the associated magnetic moment, μ_J, are quantized along the magnetic field direction into 2J+1 components, i.e. M_J = J,J-1, ..., -J. This is manifested as a Zeeman broadening of the rotational lines in an electronic spectrum. Because right and left circularly polarized light is scattered by positive and negative M_J components, respectively, the wings of a Zeeman broadened line show positive or negative rotation of the plane of polarization of transmitted light, as observed through crossed polarizers. The strength of the m.r.s. effect is determined by the magnitude of the magnetic moment, μ_J, and, since only electron orbital and electron spin angular momenta generate significant magnetic moments, only orbitally degenerate or spin multiplet electronic states give an observable magnetic rotation spectrum.

*References (51,52).